



UNIVERSITEIT•STELLENBOSCH•UNIVERSITY
jou kennisvennoot • your knowledge partner

The limitations of a continuous wave Doppler radar for vehicle speed measurement and enforcement

Johann Ruben van Tonder
22569596

Report submitted in partial fulfilment of the requirements of the module
Project (E) 448 for the degree Baccalaureus in Engineering in the Department of
Electrical and Electronic Engineering at Stellenbosch University.

Supervisor: Dr W. Steyn

November 2022

Acknowledgements

I would like to sincerely thank the following people for assisting me in my completion of my project:

- Dr. Werner Steyn who tirelessly assisted and guided me through the project. I hope to capture at least a small amount of the knowledge he shared with in this report.
- Mr. Wessel Kroukamp for assisting me in the building of my horn antenna.
- My brother, Ulrich van Tonder, and sister, Inge van Tonder, who assisted in testing my radar by driving up and down the road outside our house.
- My father, Johann van Tonder, who assisted me in building the wooden structure to which I attached my radars hardware.
- My mother, Estelle van Tonder, who also assisted me by driving up and down the road outside our house.
- The South African National Space Agency who has financially supported me this year



UNIVERSITEIT•STELLENBOSCH•UNIVERSITY
jou kennisvennoot • your knowledge partner

Plagiaatverklaring / Plagiarism Declaration

1. Plagiaat is die oorneem en gebruik van die idees, materiaal en ander intellektuele eiendom van ander persone asof dit jou eie werk is.

Plagiarism is the use of ideas, material and other intellectual property of another's work and to present it as my own.

2. Ek erken dat die pleeg van plagiaat 'n strafbare oortreding is aangesien dit 'n vorm van diefstal is.

I agree that plagiarism is a punishable offence because it constitutes theft.

3. Ek verstaan ook dat direkte vertalings plagiaat is.

I also understand that direct translations are plagiarism.

4. Dienooreenkomsdig is alle aanhalings en bydraes vanuit enige bron (ingesluit die internet) volledig verwys (erken). Ek erken dat die woordelikse aanhaal van teks sonder aanhalingstekens (selfs al word die bron volledig erken) plagiaat is.

Accordingly all quotations and contributions from any source whatsoever (including the internet) have been cited fully. I understand that the reproduction of text without quotation marks (even when the source is cited) is plagiarism

5. Ek verklaar dat die werk in hierdie skryfstuk vervat, behalwe waar anders aangedui, my eie oorspronklike werk is en dat ek dit nie vantevore in die geheel of gedeeltelik ingehandig het vir bepunting in hierdie module/werkstuk of 'n ander module/werkstuk nie.

I declare that the work contained in this assignment, except where otherwise stated, is my original work and that I have not previously (in its entirety or in part) submitted it for grading in this module/assignment or another module/assignment.

22569596	
Studentenommer / Student number	Handtekening / Signature
J.R. van Tonder	October 18, 2022
Voorletters en van / Initials and surname	Datum / Date

Abstract

English

Doppler radars are the most common method to measure the speed of a vehicle. Doppler radars are capable of measuring a vehicle's speed using the Doppler effect. The use of Doppler radars started in 1949 and has come under scrutiny with many people/institutions doubting its accuracy. The project aims to formulate the limitations of a Doppler radar in vehicle speed measurement and enforcement. The limitations were formalized and tested in ideal and non-ideal conditions. A Doppler radar can accurately measure a vehicle's speed but is confined to ideal conditions. Whenever non-ideal conditions are present the Doppler radar ultimately fails to accurately measure vehicle speed. The operation laws minimise the effects of the limitations but do not prevent all the limitations. The study proposes stricter laws in the operation of Doppler radars for vehicle speed measurements and enforcement.

Afrikaans

Doppler radars is die mees algemene metode om 'n motor se spoed te bepaal. Doppler radars meet die spoed van 'n voertuig deur gebruik te maak van die Doppler effek. Sedert 1949 is daar gebruik gemaak van Doppler radars in voertuig spoed handhawing. Die gebruik egter daarvan is ondersoek asgevolg van mense/instellings wat die akkuraatheid betwyfel. Die project bepoog om die tekortkominge van Doppler radars in voertuig spoed meting en handhawing te formuleer. Die tekortkominge is geformaliseer and getoets in ideale en nie-ideale omstandighede. 'n Doppler radar kan in ideale omstandighede baie akkuraat die spoed van 'n voertuig bepaal. Wanneer ookal nie-ideale omstandighede teenwoordig is misluk die Doppler radar om voertuig spoed lesing te neem. Die handelings wette verminder die effek van die tekortkominge, maar verhoed nie almal nie. Die studie stel voor dat die handeling van Doppler radars in voertuig spoed lesing and handhawing strenger wette moet handhaaf.

Contents

Declaration	ii
Abstract	iii
List of Figures	vii
List of Tables	x
Nomenclature	xi
1. Introduction	1
1.1. Background	1
1.2. Problem Statement	2
1.3. Objectives	2
1.4. Summary of Work	2
1.5. Scope	3
1.6. Format of Report	3
2. Literature Review	4
2.1. Proposed Doppler Radar Solutions	4
3. Radar Physics	6
3.1. Electromagnetic Wave Propagation	6
3.2. Radar Equation	7
3.3. Radar Frequencies	8
3.4. Radar Cross Section	9
3.5. CW Doppler Radar	10
3.6. Frequency Resolution	11
3.7. Range Resolution	12
3.8. Radar Clutter	13
3.9. Antenna Parameters	13
4. Limitations of a CW Doppler radar in Vehicle Speed Measurement	15
4.1. Cosine Effect	15
4.2. Accuracy and Acceleration Limits	16
4.3. Object Identification	17

4.4. Antenna Sidelobes	18
4.5. Multiple Path Reflection	19
4.6. Radar Receiver Saturation	19
5. Doppler Radar	21
5.1. System Design	21
5.1.1. Doppler Sensor	21
5.1.2. Antenna	21
5.1.3. Lowpass Filter and Amplifier	22
5.1.4. Voltage Regulator	22
5.1.5. Soundcard	22
5.1.6. Software	22
5.2. Detailed Design	23
5.2.1. Filter	23
5.2.2. Amplifier	24
5.2.3. Voltage Regulator	25
5.2.4. Clipper	25
5.2.5. Antenna	26
5.2.6. Software	27
6. Results	30
6.1. Radar and Setup	30
6.2. Radar Results	31
6.3. Results of Limitations	32
6.3.1. Results of Cosine Effect	32
6.3.2. Results of Accuracy and Acceleration Limits	32
6.3.3. Results of Object Identification	34
6.3.4. Results of Antenna Sidelobes	36
6.3.5. Results of Multiple Path Reflection	36
6.3.6. Results of Radar Receiver Saturation	37
7. Conclusion	39
7.1. Objectives	39
7.2. Operations	39
7.3. Future Work	40
Bibliography	41
A. Project Planning Schedule	43
B. Outcomes Compliance	44

C. Figures	46
D. Radar Software	49
E. Antennas	51
F. Radar Simulations	53
G. Spectrograms regarding the Accuracy and Acceleration	56
H. Spectrograms regarding the Antenna Sidelobe	58
I. Matlab Code	61

List of Figures

2.1. Proposed Doppler speed measurement configuration	4
3.1. Electromagnetic Waveform	6
3.2. A Basic Radar	7
3.3. Equivalent Sphere shape	9
3.4. CW Doppler Radar	11
3.5. Result of Frequency Mix	11
4.1. Cosine Angle β	15
4.2. Frequency Versus Time Resolution	16
4.3. Vehicle Ranges for Equal Echo Power	17
4.4. Antenna Radiation Pattern	18
4.5. Multiple Reflections	19
4.6. Intermodulation Distortion	20
5.1. System Diagram of Project	21
5.2. Filter Circuit	23
5.3. Amplifier Circuit	24
5.4. Voltage Swing Circuit	25
5.5. Voltage Reference Circuit	25
5.6. Voltage Regulator Circuit	25
5.7. Diode Clipper Circuit	26
5.8. Rectangular Waveguide	26
5.9. Horn Geometry	27
5.10. Speed Algorithm	28
6.1. Side View of Radar	30
6.2. Back View of Radar	30
6.3. Radar Setup	30
6.4. Measured Spectrogram of Vehicle	31
6.5. Speed Measured from Radar and GPS	31
6.6. Cosine Error on Vehicle Speed	32
6.7. Measured Speed with best combination of Time and Frequency Resolution	33
6.8. Measured Speed with Differentiation in Frequency	33
6.9. Measured Speed with Differentiation in Time	34

6.10. Spectrogram of Large Vehicle	34
6.11. Spectrogram of Small Vehicle	35
6.12. Spectrogram of Two vehicles in Radar Range	35
6.13. Tracked Speed of Vehicle	35
6.14. Comparison of Radiation Patterns between HB100 and Horn Antenna	36
6.15. Multiple Path Reflection Setup	36
6.16. Spectrogram of Multiple Path Reflection	37
6.17. Tracked Speed of Multiple Path Reflection	37
6.18. Spectrogram of Radar Receiver Saturation	38
6.19. Speed tracking when Saturation occurs	38
6.20. Extreme Receiver Saturation	38
A.1. Tracking Gantt Chart used for Project Planning	43
C.1. Gain versus Frequency plot of MCP602 op-amp	46
C.2. Ublox GPS Module	46
C.3. Relative Field Strength Graph	47
C.4. Homemade Billboard	47
C.5. Surface waves on micro strip copper line	48
E.1. HB100 Radiation Pattern in CST	51
E.2. HB100 3D Radiation Pattern in CST	51
E.3. Schematic Drawing of HB100 Sensor	51
E.4. Horn Antenna 1D Radiation Pattern	52
E.5. Horn Antenna 3D Radiation Pattern	52
E.6. Schematic Drawing of Waveguide	52
E.7. Schematic Drawing of Horn Antenna	52
F.1. Input and Amplified Output	53
F.2. Frequency Response of Lowpass Filter	53
F.3. LTSpice Simulation of Radar Hardware	54
F.4. Spectrogram of Simulated Signal	55
F.5. Measured Speed from Simulated Signal	55
G.1. Spectrogram with best combination of Time and Frequency Resolution	56
G.2. Spectrogram with Differentiation in Frequency	56
G.3. Spectrogram with Differentiation in Time	57
H.1. Spectrogram of Radar facing North	58
H.2. Spectrogram of Radar facing 30 Degrees West of North	58
H.3. Spectrogram of Radar facing 60 Degrees West of North	59
H.4. Spectrogram of Radar facing 0 Degrees West of North	59

H.5. Spectrogram of Radar facing 30 Degrees West of North	59
H.6. Spectrogram of Radar facing 60 Degrees West of North	60

List of Tables

2.1. Accuracy Comparison from HB100 Sensor	5
3.1. Standard Microwave Frequency letter-band nomenclature	9
3.2. Doppler Shift as a Function of Velocity and Frequency	12
4.1. Estimates of vehicle RCS	17
6.1. Comparison between Sample Sizes	34
6.2. Measurable Distance of Radar	36
7.1. Response to Objectives	39

Nomenclature

Variables and functions

E	Electric
H	Magnetic
B	Magnetic Flux Density
μ	Permeability
ϵ	Permittivity
R	Range
G	Gain
V	Voltage
I	Current
P	Power
P_t	Transmitter Power
P_d	Power Density
P_r	Received power
σ	Radar Cross section
λ	Wavelength
A_e	Receive Aperture
τ	Dwell Time
c	Speed of light
f	Frequency
τ_p	Pulse width
t_i	Measurement Time
I_r	Reflected Intensity
I_i	Incident Intensity
w	Angular Frequency
ϕ	Phase

Variables and functions

f_o	Generated Frequency
f_d	Doppler Frequency
v	Vehicle Velocity
N_f	Fast Fourier Transform Size
B	Bandwidth
S_r	Range Resolution
P_o	Input Power
U	Radiation Intensity
N	Sample Size

Acronyms and abbreviations

RADAR	Radio Detection and Ranging
CSIR	Council for Scientific and Industrial Research
PBY	Patrol Bomber Y
CW	Continuous Wave
FMCW	Frequency Modulated Continuous Wave
RCS	Radar Cross Section
SNR	Signal to noise ratio
NBF	Narrow band filter
FFT	Fast Fourier transform
DFT	Discrete Fourier transform
STFT	Short time Fourier transform
RC	Resistor and Capacitor
ADC	Analog to Digital Converter
AGC	Automatic Gain Control
RMS	Root Mean Squared
GNSS	Global Navigation Satellite System
NMEA	National Marine Electronic Association
PC	Personal Computer
OP-AMP	Operational Amplifier
DC	Direct Current
AC	Alternating Current
TE	Transverse Electric
TM	Transverse Magnetic

Chapter 1

Introduction

1.1. Background

The traditional way of measuring vehicle speeds is done with the well-known phenomenon called the Doppler effect. Doppler radars were invented in the second world war, by John L. Barker Sr. and Ben Midlock [1]. They were tasked with solving the problem of terrestrial landing gear damage on the now legendary aircraft the PBY Catalina [2]. Barker and Midlock attached a Doppler radar unit, made out of coffee cans soldered shut to act as microwave resonators, to the end of the runway to measure the sink rate of landing PBYs. The radar gun was later used in 1947 by the Connecticut State Police in Glastonbury, Connecticut. After two years of testing and surveying in 1949, the state police began issuing speed tickets. Over the years the use of Doppler radar guns has come under some scrutiny. In 1987, the CSIR did their independent case study [3] on the validity of Doppler radars for vehicle speed measurements. The case study reported that there are several limitations in vehicle speed measurements, but most importantly the limitation that posed the greatest threat is identifying which vehicle is supplying the measurement. Knowing these limitations might limit the error in vehicle speed measurements and improve accuracy. Establishing how accurate Doppler radars are in vehicle speed measurements might give rise to a change in how vehicle speed is enforced. The goal is to increase safety on roads and limit accidents while making sure the right person is punished for speeding. Below are the operation parameter prescribed by law when using Continuous-Wave(CW) Doppler radars to measure vehicle speed in South Africa [4],

- No metal road signs or vertical flat surfaces larger than 1 meter in vertical height within 15° on either side of the aiming direction, within a distance of 200 m of the antenna.
- No signals received and processed from vehicles more than 500 meters away
- No other moving vehicle other than the measured vehicle within 600 meters from the radar in the direction of operation
- The vehicle's speed should be tracked for 3 s for a valid reading to be possible

1.2. Problem Statement

The objective of the report is to determine the limitations of a CW Doppler radar in vehicle speed measurement and if the prescribed operating laws are sufficient in mitigating these limitations.

1.3. Objectives

1. Identify the possible limitations of CW Doppler radars in vehicle speed measurements
2. Develop hardware for a CW Doppler radar that can perform up to 80 m
3. Develop software capable of calculating the speed of targets
4. Develop software capable of tracking a vehicle
5. The radar should be able to distinguish between a vehicle and clutter
6. Test the theorized limitations of CW Doppler limitations in vehicle speed measurements
7. Determine whether the laws and regulations are satisfactory in limiting possible errors and limitations

1.4. Summary of Work

Research was conducted to first understand how radars work. A thorough understanding was gathered how the radar equation is formulated and how CW Doppler radar differs from other radars. After establishing how a CW Doppler radar is capable of measuring a vehicles speed. The limitations of a CW Doppler radar in vehicle speed measurement was formulated with the knowledge obtained and further research.

To practically test the limitations a CW Doppler radar in vehicle speed measurement, a radar was built. The radar was built with a combination of self designed hardware and sensor integration. The accompanying radar software was designed in Matlab, this was also where all the data processing was done. The radar was tested against GPS speed data to estimate its accuracy before testing the identified limitations. The limitations was then tested and then represented in such a way to clearly indicate where a CW Doppler radar performs accurately and where not. Lastly a comparison was made between the identified and tested limitations, and the operating laws of a CW Doppler radar.

The conclusion was drawn that although a CW Doppler radar is capable of accurately measuring the speed of a vehicle, its accuracy is limited to only one vehicle moving in its range. There are many cases where a CW Doppler radar is unable to determine a specific vehicle's speed. The biggest limitation of a CW Doppler radar comes down to its inability to determine which vehicle is traveling at which measured speed, in the case that two or more vehicles are in range. The operating laws mitigate these limitations to some extent but fail to completely resolve them.

1.5. Scope

The project scope is to determine the limitations of a CW Doppler radar in vehicle speed measurement. The project does not entail the design of a CW Doppler radar and/or how design choices might affect the radar. This project rather focused on building a suitable radar that would demonstrate the limitations of a CW Doppler radar in vehicle speed measurement. A moving CW Doppler radar is not considered in this project.

1.6. Format of Report

- **Chapter 2** discusses other notable work on Doppler radars and their application to vehicle speed measurements. This is also where the differentiation is made to how this project differs from previous work.
- **Chapter 3** starts with the introduction to radar physics. It then proceeds to discuss the formulation of the radar equation and fundamental concepts of a CW Doppler radar.
- **Chapter 4** formulates the limitations of CW Doppler radars in vehicle speed measurement.
- **Chapter 5** discusses the design choices and options considered for the CW Doppler radar. The chapter also contains the detailed design of the CW Doppler radar.
- **Chapter 6** presents the accuracy of the CW Doppler radar. The chapter then proceeds to discuss how the formulated limitations were tested and draws a conclusion from the results of the tests.
- **Chapter 7** concludes whether the operation laws successfully deter the limitations of a CW Doppler radar and points to future work.

Chapter 2

Literature Review

2.1. Proposed Doppler Radar Solutions

A proposed solution to the problem of vehicle identification was developed by Neil Cameron Martin [5] published in 1987, where the proposed system shown in Figure 2.1, indicates the use of two sources to measure and compare their results. For example, source one only measures vehicle speeds of B and C and source two only measures vehicle speeds of A and C. The configuration will allow you to determine which vehicle is travelling at what speed. The thesis concluded that the system improved the reliability of identifying which vehicle is travelling at what speed. Unfortunately, this system has not been adopted into law enforcement speed regulations. Leaving the case study of the CSIR still at the heart of the problem. This might be due to the complex real-time processing required at the time to successfully implement the system.

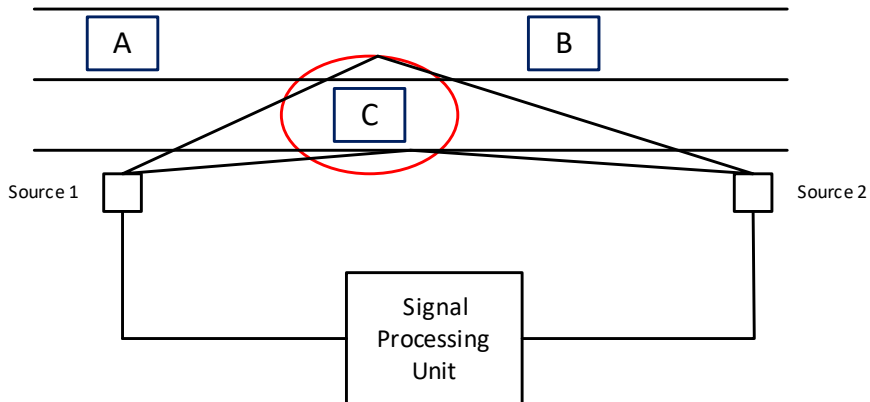


Figure 2.1: Proposed Doppler speed measurement configuration

Other noteworthy work was done by Nguyen Giang Lam [6]. Nguyen focussed on developing a Doppler radar with an HB100 X-band sensor [7]. To quite some success Nguyen developed the sensor with an ESP-32 microcontroller module. The developed system was capable of measuring speeds close to the speed measured from the vehicle, shown in Table 2.1. The measurement was only attained from a distance of 15 m. Nguyen's work focused on building a functional Doppler radar and he did not focus on the limitations of a Doppler radar.

Table 2.1: Accuracy Comparison from HB100 Sensor

Speed from the car	Speed from the HB100 Sensor
0 Km/h	0 Km/h
10 Km/h	11 Km/h
17 Km/h	16 Km/h
20 Km/h	20 Km/h
25 Km/h	24 Km/h
30 Km/h	31 Km/h
35 Km/h	35 Km/h

Apart from the CSIR case study, which is only referenced in Neil Cameron Martin's masters dissertation, there is very little information on how big an influence certain limitations of a Doppler radar have on vehicle speed measurements. In my project, I will aim to adapt the system design by Nguyen to measure vehicles from as far as 80 m and instead of real-time processing I will instead focus on recording data and then applying different processing methods to illustrate the formulated limitations, that is discussed in Chapter 4.

Chapter 3

Radar Physics

3.1. Electromagnetic Wave Propagation

The principle that allows radars to work stems from Maxwell's equation. Maxwell derived his electromagnetic wave equation from the corrected Ampère's circuit law shown in equation 3.1 and 3.2. Faraday's law of induction is shown in equation 3.3 and 3.4.

$$\nabla \cdot E = 0 \quad (3.1) \qquad \nabla \times E = -\frac{\partial B}{\partial t} \quad (3.2)$$

$$\nabla \cdot B = 0 \quad (3.3) \qquad \nabla \times B = \mu\epsilon \frac{\partial E}{\partial t} \quad (3.4)$$

Maxwell derivation is today replaced by combining Ampère's and Faraday's to obtain the electromagnetic wave equation in a vacuum shown in equation 3.5 and 3.6, known as the wave equation.

$$\frac{1}{\sqrt{\mu\epsilon}} \frac{\partial^2 E}{\partial t^2} - \nabla^2 E = 0 \quad (3.5) \qquad \frac{1}{\sqrt{\mu\epsilon}} \frac{\partial^2 B}{\partial t^2} - \nabla^2 B = 0 \quad (3.6)$$

The electromagnetic waveform is generated by a periodic change in the current inside an antenna. The waveform that is generated from the antenna is indicated in Figure 3.1, the blue waveform is the E-field, which is perpendicular to the red waveform, which is the H-field. The waveform propagates in the z-direction.

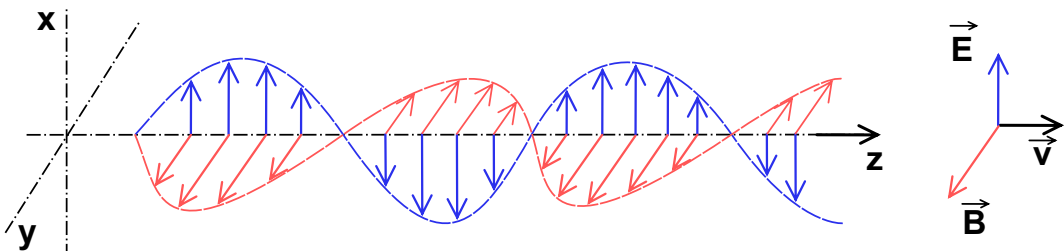


Figure 3.1: Electromagnetic Waveform

Consider the basic radar illustrated in Figure 3.2, it is an antenna transmitting an electromagnetic wave, the waveform then propagates through the air until it reaches a target. A portion of the transmitted energy is intercepted by the target and is scattered, some of it in the direction of the radar, where it is collected by the receiving antenna.

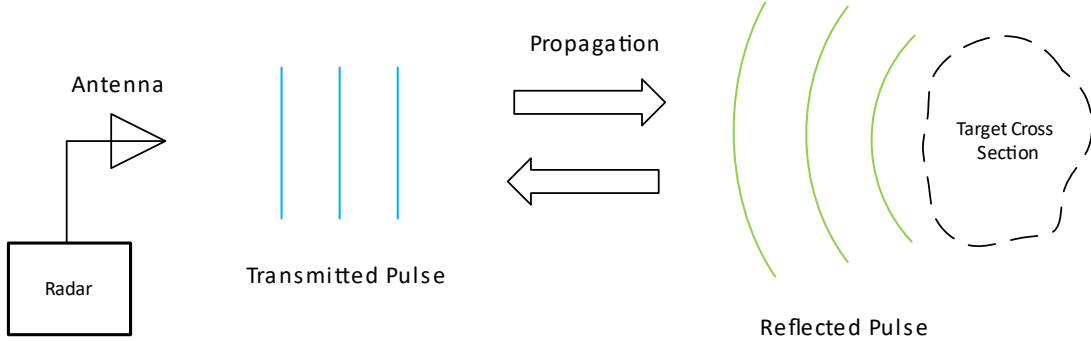


Figure 3.2: A Basic Radar

3.2. Radar Equation

The radar equation relates the range of radar to the characteristics of the transmitter, receiver, target and environment [8]. Understanding the radar equation not only gives you a means for determining the maximum distance from the radar to the target but can also serve as a tool for understanding radar operation and radar design. If the power of the radar transmitter is denoted by P_t , and if an isotropic antenna [9], one which radiates uniformly in all directions, is used. The power density P_d at a distance R from the radar is equal to the transmitter power divided by the surface area $4\pi R^2$ of an imaginary sphere of radius R , the power density is given by

$$P_d = \frac{P_t}{4\pi R^2} \quad (3.7)$$

When the radar employs a directive antenna to channel or direct the radiated P_t into some particular direction. The gain G of an antenna is a measure of the increased power radiated in the direction of the target as compared with the power that would have been radiated from an isotropic antenna. This means P_d at the target from an antenna with transmitting gain G is

$$P_d = \frac{P_t G}{4\pi R^2} \quad (3.8)$$

A portion of the radiated power is intercepted by the target and reradiated in various directions. The measure of the amount of incident power intercepted by the target and reradiated back towards the radar is denoted by the radar cross section σ , and is defined by the relation

$$P_d = \frac{P_t G}{4\pi R^2} \frac{\sigma}{4\pi R^2} \quad (3.9)$$

The radar cross-section σ has units of area. It is a characteristic of the particular target and is a measure of its size as seen by the radar. The radar antenna captures a portion of the echo power. If the effect is denoted by A_e , the power P_r , received by the radar is

$$P_r = \frac{P_t G A_e \sigma}{(4\pi)^2 R^4} \quad (3.10)$$

The maximum range of the radar R_{max} is the distance beyond which the target cannot be detected. It occurs when the received signal power P_r , just equals the minimum detectable signal S_{min} . Therefore

$$R_{max} = \left(\frac{P_t G A_e \sigma}{(4\pi)^2 S_{min}} \right)^{\frac{1}{4}} \quad (3.11)$$

Antenna theory gives the relationship between the transmitting gain and the receiving effective area of an antenna as

$$G = \frac{4\pi A_e}{\lambda^2} \quad (3.12)$$

Generally, radars use the same antenna for transmitting and receiving by substituting equation 3.12 into equation 3.11, resulting in

$$R_{max} = \left(\frac{P_t (A_e)^2 \sigma}{4\pi (\lambda)^2 S_{min}} \right)^{\frac{1}{4}} \quad (3.13)$$

3.3. Radar Frequencies

Radars conventionally operate at frequencies from 220 MHz to 35 GHz. These are not limits but rather standards proposed by the International Telecommunications Union [10]. Early in the development of radar, a letter code such as S, X, L, etc., was employed to designate radar frequency bands. The original purpose was to safeguard military secrecy, and the designation was maintained. The frequency band of importance for a Doppler radar are referred to as the Microwave region. The Microwave region ranges from 300MHz to about 36 GHz. Table 3.1 shows the designated bands inside the Microwave region.

Table 3.1: Standard Microwave Frequency letter-band nomenclature

Band Designation	Nominal Frequency range (GHz)
<i>UHF</i>	0.3-1
<i>L</i>	1-2
<i>S</i>	2-4
<i>C</i>	4-8
<i>X</i>	8-12
<i>K_u</i>	12-18
<i>K</i>	18-27

Doppler radars are operated in the *X*-band region, this is mainly due to law enforcement from the mid-1950s [11]. The reason behind using *X*-band as opposed to *K*-band or *K_u*-band is due to *X*-band being less affected by poor weather conditions. There are however disadvantages when using *X*-band over *K*-band, *X*-band requires a larger antenna and is easy for radar detectors to pick up at long distances. The operating frequency is related to the wavelength as shown below

$$\lambda = \frac{c}{f} \quad (3.14)$$

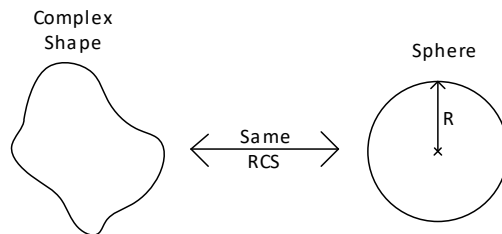
The higher the frequency, the smaller the wavelength. Meaning the radar will be able to measure smaller details the higher its operating frequency is.

3.4. Radar Cross Section

The radar cross-section (RCS) [12], is a measure of the reflectivity of an object and is formulated as

$$\sigma = \lim_{R \rightarrow \infty} 4\pi R^2 \frac{I_r}{I_i} \quad (3.15)$$

where I_r is the reflected intensity and I_i is the incident intensity. The $4\pi R^2$, comes from the assumption, that the radar cross-section is assumed to take the shape of a sphere, this assumption is illustrated below

**Figure 3.3:** Equivalent Sphere shape

Most of the incident energy is scattered and only a small fraction is reflected on the radar. Larger objects usually, but not always, have larger reflections and a longer radar

detection range R . The object parameters that influence the RCS are size, shape and reflectivity [13]. Flat surfaces reflect energy better than contoured shapes. Edges with diameters on the order of a wavelength of the radar frequency tend to be good reflectors. All metals and alloys are excellent reflectors at all frequencies. Metal screens with gaps spacing less than a quarter wavelength are as reflective as solid surfaces. Composites, fibreglass and plastic are bad reflectors at microwave frequencies.

3.5. CW Doppler Radar

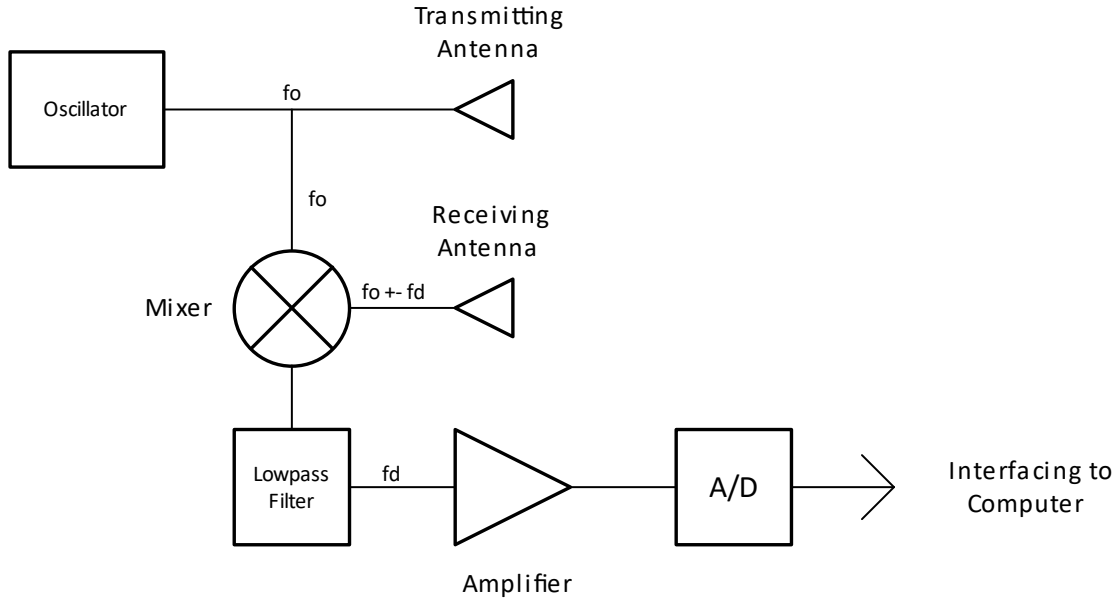
It is well known in the fields of optics and acoustics that if either the source of oscillation or the observer of the oscillation is in motion, an apparent frequency shift will result. This is known as the Doppler Effect and is the basis of CW Doppler Radar [8]. If the distance between the radar and target is R , the total number of wavelengths λ contained in the two-way path between the radar and target is $\frac{2R}{\lambda}$. Since one wavelength corresponds to an angular excursion of 2π radians, the total angular excursion ϕ made by the electromagnetic wave during its transit to and from the target is $\frac{4\pi R}{\lambda}$ radians. If the target is in motion, R and the phase ϕ are continually changing. A change in ϕ with respect to time is equal to a frequency. This is the Doppler angular frequency ω , given by equation 3.16

$$2\pi f_d = \omega = \frac{4\pi \partial R}{\partial t} = \frac{4\pi v}{\lambda} \quad (3.16)$$

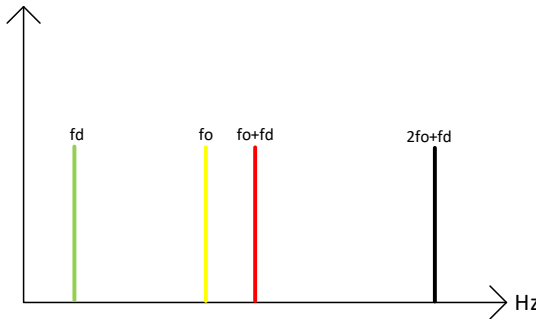
where f_d = Doppler frequency shift and v = relative velocity of target with respect to radar. The Doppler frequency shift is given by equation 3.17

$$f_d = \frac{2v}{\lambda} = \frac{2vf_o}{c} \quad (3.17)$$

where c is the speed of light in a vacuum. Consider the CW Doppler radar as illustrated in Figure 3.4. The oscillator generates a continuous frequency f_o , which is transmitted by the antenna. If the target is in motion with velocity v , relative to the radar, the received signal will be shifted in frequency from the transmitted frequency f_o , by an amount $\pm f_d$, given by equation 3.17. The plus sign associated with the Doppler frequency applies if the distance between the radar and target decreases. The minus sign applies if the distance is increasing. The received echo signal at frequency $f_o \pm f_d$, enters the radar via the antenna and is heterodyned in the mixer, with the transmitted signal f_o to produce a Doppler beat note of frequency f_d . This is illustrated in Figure 3.5, note that the sign of f_d is lost in the process.

**Figure 3.4:** CW Doppler Radar

The resulting Doppler frequency obtained from the mixer is then passed through a lowpass filter, to filter out all the frequency components above f_d . The signal is then amplified before its sampled by an analogue-to-digital converter and then passed on to the computer interface for signal processing and analysis.

**Figure 3.5:** Result of Frequency Mix

3.6. Frequency Resolution

Doppler frequency resolution is the ability to distinguish between two objects travelling at different speeds, but at the same distance from the radar. Frequency resolution is inversely related to the dwell time, the time an antenna spends on a target. The greater the dwell time the finer the frequency resolution

$$\Delta f_D = \frac{1}{\tau} \quad (3.18)$$

We can also estimate the Doppler accuracy as, where SNR is the signal to noise ratio

$$\delta f_D = \frac{\Delta f_D}{t\sqrt{2SNR}} \quad (3.19)$$

To plot the spectrum of the sampled signal individual narrow band filters(NBF) must be as narrow as possible in bandwidth to allow accurate Doppler measurements and minimize the amount of noise power. In theory, the operating bandwidth of a CW Doppler radar is infinitesimal. However systems with infinitesimal bandwidths cannot physically exist and thus, the bandwidth of CW Doppler radars is assumed to correspond to that of a gated CW waveform.

An NBF bank can be implemented using a Fast Fourier Transform(FFT). If the Doppler filter bank is implemented using FFT of size N_f , and if the individual NBF bandwidth is Δf_D , then the effective radar Doppler bandwidth is

$$B = N_f \Delta f_D \quad (3.20)$$

The table 3.2 below indicates the Doppler shift as a function of velocity and frequency [14].

Table 3.2: Doppler Shift as a Function of Velocity and Frequency

<i>f</i>		Doppler Shift f_D (Hz)	
Band	Frequency (GHz)	1 m/s	1km/h
<i>L</i>	1	6.67	1.85
<i>S</i>	3	20	5.55
<i>C</i>	5	33.3	9.25
<i>X</i>	10	66.7	18.53
<i>K_u</i>	16	107	29.72
<i>K_a</i>	35	233	64.72

3.7. Range Resolution

The range resolution of a radar is its ability to distinguish between two or more targets on the same bearing, the angle measured relative to a hypothetical north, but at different ranges [15]. The degree of range resolution depends on the width of the transmitted pulse τ_p , the types and sizes of targets, and the efficiency of the receiver. Pulse width τ_p is the primary factor in range resolution. The simplified theoretical range resolution can be calculated from

$$S_r = \frac{c\tau_p}{2} \quad (3.21)$$

An unmodulated CW Doppler radar does not have range resolution. To acquire range resolution some sort of timing mark must be applied to a CW carrier if the range is to be measured. The timing mark permits the time of transmission and the time of return to be recognized. The more distinct the mark, the broader the transmitted spectrum will be. This follows from the properties of the Fourier transform,

$$\mathfrak{F}(h(t)) = \int_{-\infty}^{\infty} h(t) e^{-j2\pi f_t t} dt \quad (3.22)$$

therefore a finite spectrum must be transmitted if transmit time or range is to be measured. The spectrum of a CW transmission can be broadened by the application of modulation either amplitude, frequency or phase. A widely used technique is to frequency-modulate the carrier resulting in a Frequency Modulated Continuous-Wave(FMCW).

3.8. Radar Clutter

Land clutter is difficult to quantify and classify. The clutter is widely dependent on the type of terrain, as described by its roughness and dielectric properties. Buildings, towers, and other structures give more intense echo signals than forests and vegetation because of the presence of flat reflecting surfaces. Land clutter will mostly affect the targets with small radar cross-sections, like motorcycles. Birds flying past a radar are also seen as a type of clutter.

3.9. Antenna Parameters

The purpose of the antenna is to act as a transducer between free-space propagation and guided-wave (transmission-line) propagation. The function of the antenna during transmission is to concentrate the radiated energy into a shaped beam which points in the desired direction in space. On reception, the antenna collects the energy contained in the echo signal and delivers it to the receiver. Antenna design and theory are very complex. To understand the application of an antenna in radars there are two pieces of theory to understand, namely Gain and Directivity.

Gain is a measure of the ability of the antenna to direct the power delivered to the input into radiation in a particular direction. Gain is measured at the peak radiation intensity. Consider the power density radiated by an isotropic antenna at a distance R and input power P_t :

$$P_d = \frac{P_0}{4\pi R^2} \quad (3.23)$$

As isotropic antenna radiates equally in all directions and the power density P_d is found by dividing the radiated power by the area of the sphere with radius R . The isotropic

radiator is considered to be 100% efficient. The gain of a real antenna increases the power density in the direction of the peak radiation.

$$P_d = \frac{P_t G}{4\pi R^2} \quad (3.24)$$

Directivity is a measure of the concentration of the radiation in the direction of the maximum radiation. Directivity is the maximum radiation intensity over the average radiation intensity:

$$\text{Directivity} = \frac{U_{max}}{U_{avg}} \quad (3.25)$$

Directivity and gain differ only by efficiency, but the directivity is easily estimated from patterns. Gain, directivity times efficiency, must be measured. The average radiation intensity can be found from a surface integral on the radiation sphere of the radiation intensity divided by 4π , the area of a sphere in steradians.

$$U_{avg} = \frac{1}{4\pi} \int_0^{2\pi} \int_0^\pi U(\theta, \phi) \sin\theta d\theta d\phi \quad (3.26)$$

Chapter 4

Limitations of a CW Doppler radar in Vehicle Speed Measurement

4.1. Cosine Effect

The incorrect Doppler frequency is measured from the radar when the vehicle is not travelling directly towards the radar, this is illustrated in figure 4.1. The phenomenon is called the Cosine Effect because the measured speed is directly related to the cosine angle between the radar and the vehicle's direction of travel. The cosine angle is calculated by the equation below,

$$\beta = \tan^{-1}\left(\frac{d}{R}\right) \quad (4.1)$$

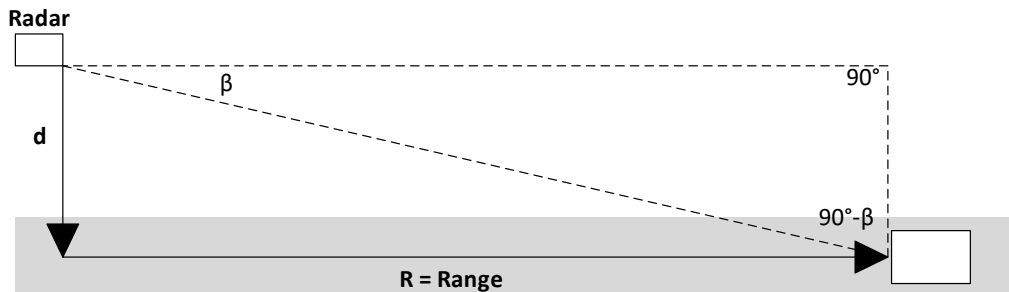


Figure 4.1: Cosine Angle β

The error in speed measurement is calculated in equation 4.2, where β is the incident angle, R target range to radar and d is the antenna distance to the middle of the target lane. As the target lane becomes curved or the radar is placed in the air the change in angle is too great for the radar to give an accurate result. Below is the equation for correcting the cosine error,

$$V_m = V_o \cos(\beta) = V_o \frac{R}{(R^2 + d^2)^{0.5}} \quad (4.2)$$

V_m is the measured speed and V_o the actual speed. As highlighted in section 3.7 the CW Doppler radar cannot determine how far away a target is from the radar. There

are some software techniques you can apply, but their accuracy is questionable. The measured speed will always be less than the actual speed and thus care should be taken when enforcing minimum speed limits.

4.2. Accuracy and Acceleration Limits

Under ideal conditions, most speed measurement radars should have an accurate reading of about ± 1 km/h. A very important part of radar is to discriminate between different frequency components in a signal, in a short period. Radars are capable of extracting frequency from the measured values of an Analog-To-Digital Conversion(ADC) by a Discrete Fourier Transform(DFT) analysis of nonstationary signals. Nonstationary signals are signals that differ in frequency over time. To differentiate between frequency components a short period of the signal is used to calculate the frequency spectrum, hence the name Short Time Fourier Transform(STFT). The sample taken in the time domain has a trade-off in the frequency domain. To understand this trade-off you need to understand how the DFT works. The equation below shows how the DFT is calculated.

$$H[k] = \sum_{n=0}^{N-1} h[n]e^{-j2\pi kn/N} \quad (4.3)$$

The DFT takes a finite amount of samples, N , to calculate the frequency spectrum of discrete signal h . To increase the resolution in the frequency domain one can decrease the sampling frequency or increase frame size. To increase the resolution in the time domain you can increase the sampling frequency or decrease the frame size. Both methods have trade-offs, by increasing the frequency resolution you are decreasing the time resolution. To visualize the effect the results of a DFT are represented in a spectrogram, which has time displayed on the horizontal axis, frequency on the vertical axis and spectral magnitude displayed on the third axis by colour. Figure 4.2 illustrates the trade-off between time and frequency, the first graph highlights how to differentiate between frequency components you will lose the ability in the time domain. The right-sided graph demonstrates the opposite, to differentiate in time you lose the ability to differentiate in the frequency domain.

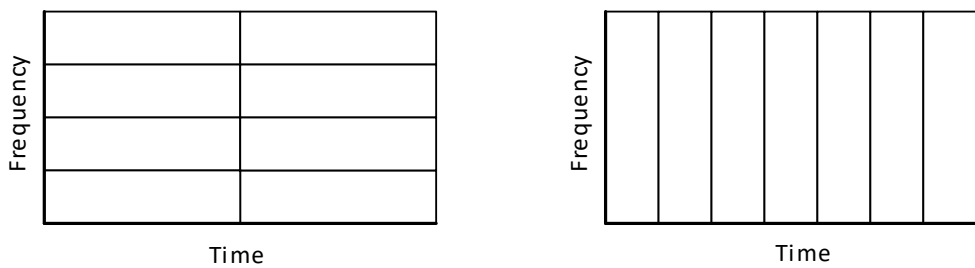


Figure 4.2: Frequency Versus Time Resolution

4.3. Object Identification

A CW Doppler radar uses the frequency spectrum to identify objects. As shown in Table 3.2, the frequency shift measured is a direct indication of how fast an object is moving. This is a very sound method and is capable of very accurate measurements. There is a problem nonetheless, how does the radar identify which object is travelling at what speed? For the case of a CW Doppler radar which does not have range resolution, discussed in section 3.7. A CW Doppler radar cannot distinguish between multiple vehicles/objects travelling at different speeds, both in the range of the radar. Due to Automatic Gain Control(AGC), discussed in section 5.1.3, being applied to the measured signal frequencies. The assumption of the closest object will generate the strongest signal is not true.

In Table 4.1 the estimate of vehicle RCS is illustrated. For motorists their RCS is relatively small, the motorcycle RCS normalised to a full-size pickup is 0.05 m^2 . This means that a motorcycle is very likely to be mistaken for a more distant vehicle. Figure 4.3, illustrates this phenomenon.

Table 4.1: Estimates of vehicle RCS

Vehicle Type	Radar Cross Section
Recreation Vehicle	400 m^2
Full Size Pickup	200 m^2
Large Car	120 m^2
Medium Size Car	60 m^2
Small Car	30 m^2
Motorcycle	10 m^2
Bicycle	5 m^2

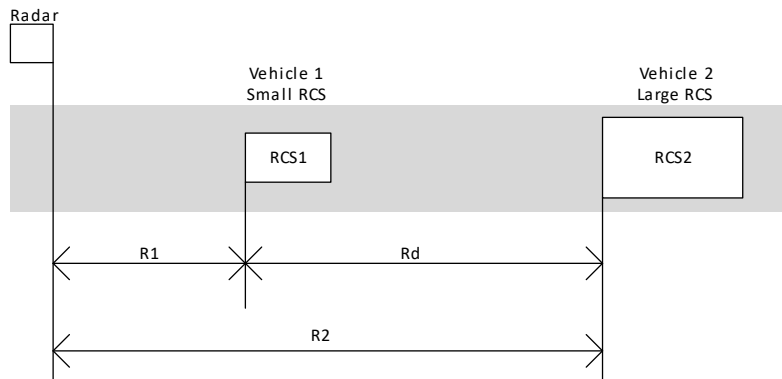


Figure 4.3: Vehicle Ranges for Equal Echo Power

The distance from the radar to the vehicle where the reflected power of vehicle two is equal to the reflected power of vehicle one, can be calculated by

$$R2 = R1 \left(\frac{\sigma_2}{\sigma_1} \right)^{\frac{1}{4}} \quad (4.4)$$

The equation can be written in terms if the distance between the two vehicles Rd ,

$$Rd = R1 \left[\left(\frac{\sigma_2}{\sigma_1} \right)^{\frac{1}{4}} - 1 \right] \quad (4.5)$$

Not only will the radar struggle to distinguish the travelling speeds of multiple vehicles in its range but it would also not be able to detect what the object is, that recorded the speed measurement. For instance, birds flying past the radar may cause false speed readings. This is not a likely phenomenon if it is just one bird due to a bird's RCS being usually around 0.1 m^2 . But when a swarm of birds fly past a radar it will cause the radar to have a false reading.

4.4. Antenna Sidelobes

An Antenna radiation pattern is a visual representation of the radiation emission from an antenna. Figure 4.4 illustrates how this can be plotted in polar coordinates. The main lobe is directed in the direction of the intended measurement. The side lobes are relatively small compared to the main lobe. This specific antenna's radiation pattern is very good to measure only in one direction/lane. This is not always the case, some antennas might have very big side lobes. This will cause the radar to measure unintended objects that are not in the direction of measurement. Attention should be applied to the antenna radiation pattern when operating the radar.

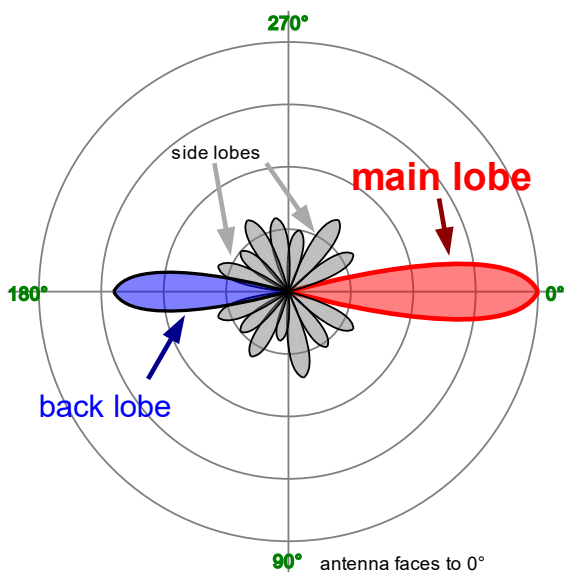


Figure 4.4: Antenna Radiation Pattern

Looking at the antenna radiation pattern of the HB100 sensor shown in figure E.1, the

antenna is not very directional. When applying AGC to the received signals, it further complicates the process. This adds to the confusion of not knowing what object is reflecting the signal. Combining antenna radiation, side lobes, and AGC. It can compromise the credibility of a radar. It is important to know the radiation pattern of your radar for both the transmitting and receiving antenna otherwise, you will not have accurate readings.

4.5. Multiple Path Reflection

The transmitted signal does not always take a direct path from radar to target and back. Any metal object, which is a good reflector, may lead to another path of reflection for the radar to measure. The radar is not capable of detecting how a signal has travelled from and back to the radar. A common object like an overhead or off-road highway sign can cause signals to reflect in multiple ways. Figure 4.5 shows two reflection paths the radar will measure when an overhead sign is placed on a highway.

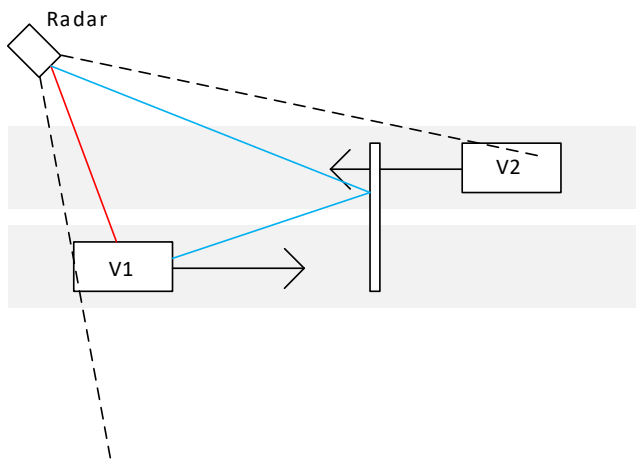


Figure 4.5: Multiple Reflections

The above illustration is just one example. There are more examples that are not as easy to quantify.

4.6. Radar Receiver Saturation

Strong echoes from larger vehicles close to the radar will reduce the radar detection range. The receiver will saturate and will not be able to measure any other vehicles in the radar range. Strong signals that saturate the radar receiver's low noise amplifier or mixer will produce cross-modulation products. Cross modulation, also known as intermodulation, is the amplitude modulation of signals containing two or more different frequencies. The intermodulation between frequency components will result in additional components at frequencies that are not just at harmonic frequencies but also the sum and difference

frequencies of multiples of those frequencies. Figure 4.6 illustrates how intermodulation can result in distortion and how this might saturate the radar receiver.

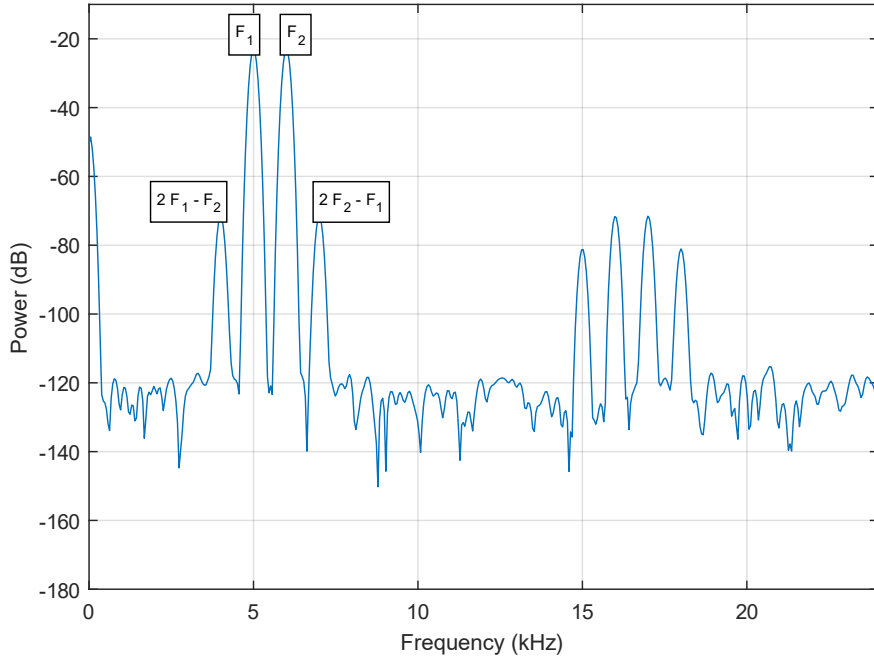


Figure 4.6: Intermodulation Distortion

To combat this some radars are equipped with AGC, to protect the receiver from signal saturation. The AGC reduces radar sensitivity but as mentioned in section 4.4 causes other problems to arise.

Chapter 5

Doppler Radar

5.1. System Design

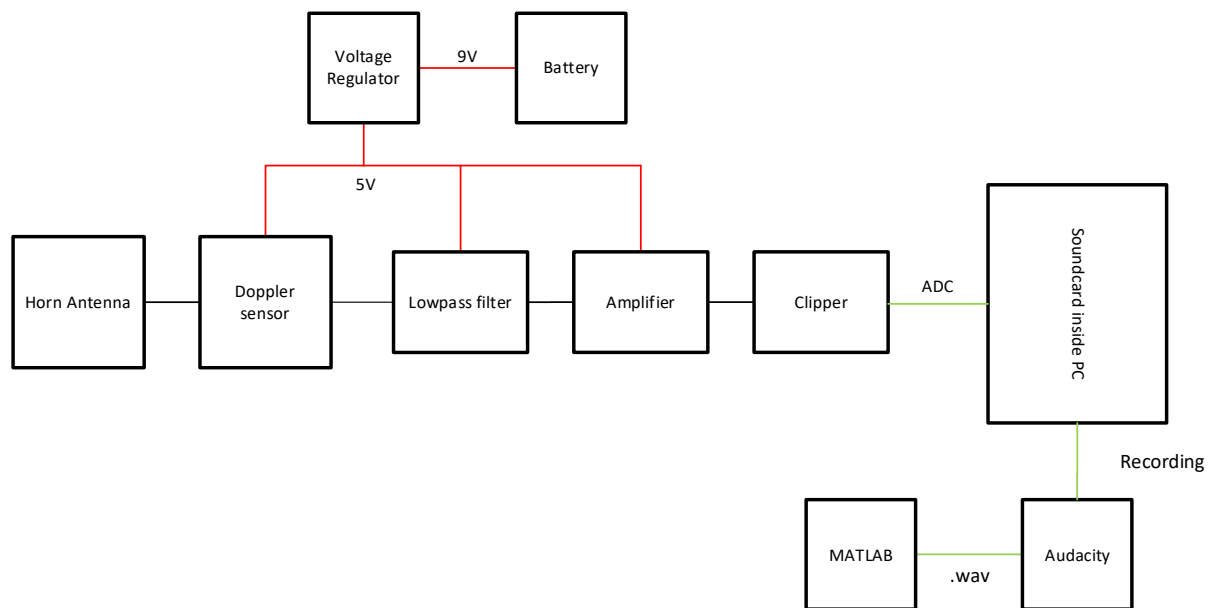


Figure 5.1: System Diagram of Project

5.1.1. Doppler Sensor

The HB100 sensor will be used for sensing the Doppler frequency. The sensor operates at 10.525 GHz and is designed for velocity measuring. The sensor includes an oscillator, mixer, transmit and receive antenna. The sensor can be operated in CW or FMCW mode. The radiation pattern of HB100 is illustrated in Figure E.1. The sensor requires a lowpass filter and amplifier before it can be sampled for analysis, this is discussed in Section 5.1.3. Another option was to build a sensor from individual components, but this is not within the scope of the project, due to its complexity.

5.1.2. Antenna

The patch antenna on the HB100 sensor is shown in Figure E.3. A horn antenna will be used to focus the radiation and increase the gain. The increase in antenna gain will

increase the range of the CW Doppler radar. The horn antenna was designed in CST and is illustrated in figure E.4 and E.5.

5.1.3. Lowpass Filter and Amplifier

The lowpass filter will be a second-order RC circuit, due to its simplicity. Active filters were considered but did not provide any advantage over a passive filter. The amplification of the sensor output proved to be a bit more tedious. Due to little information available on the HB100 sensor and the uncertainty of the output voltage. The only information about output levels, were that it is in the range of a few mV [16]. The amplification will be done with Operation Amplifier(op-amp), another form of amplification is AGC. AGC is when the different frequency components will be amplified and attenuated depending on their amplitude, with the goal to have all the components at the same amplitude. This will deter components that might over saturate a radar but will add complexity when determining what signal is closest to the radar. AGC was considered but the required hardware was not available. The amplification will be tested and adapted as needed to sufficiently amplify the signal. To protect the soundcard of the laptop which has ADC voltage limits of 1 V_{rms} , the output signal needs to be clipped through a diode clipper circuit at 1 V.

5.1.4. Voltage Regulator

The choice of power supply is a linear voltage regulator. Another considered option was a switched-mode power supply. Switched mode power supply has a couple of advantages over linear voltage regulators, but it produces significantly more noise compared to linear voltage regulators. The noise might affect the HB100 sensor and due to the advantages of switched mode not being utilized in my project, I decided to go with linear voltage regulators.

5.1.5. Soundcard

The soundcard inside a PC will be used to sample the Doppler sensor. The soundcard is capable of sampling at a range of frequencies from 8 kHz to 44 kHz. The Doppler frequency that I expect to sample will not exceed 3 kHz. The input limit is around 1 V_{rms} and thus the amplification is designed with this limitation taken into account.

5.1.6. Software

The sampled signal from the soundcard will be recorded in Audacity [17], which is open-source audio software. The recorded file will then be exported as a .wav file and further analyzed in Matlab. In Matlab the radar software algorithms will be coded to determine

vehicle speed, noise levels and to track a vehicle. A GPS unit will be placed inside the car used for testing the system, which will help with calibrating the system and used for comparison in non-ideal conditions. The GPS unit is a Ublox, GNSS smart board [18], with an external antenna to improve accuracy illustrated in C.2. The NMEA data strings that will be recorded in the Ublox software, will be copied to a text file and the speed extracted in Matlab.

5.2. Detailed Design

5.2.1. Filter

Due to the low Doppler frequency expected to be measured from the HB100 sensor, a second-order RC filter will result in good attenuation at higher frequencies. The cut-off frequency is calculated by equation 5.1. The Doppler frequency will not exceed 3 kHz. The second-order RC filter has a gain of 0.707^n , where n equals the number of stages. The gain will therefore be 0.5 and thus this should be considered when designing the amplifier. The values of the resistors and capacitors are chosen to be equal, $R_1=R_2$ and $C_1=C_2$. The capacitor value is chosen to be 10 nF and the resistors value 1 k Ω , due to availability of components. The -3 dB cut-off frequency is calculated to be 15 kHz.

$$f_c = \frac{1}{2\pi\sqrt{R_1C_1R_2C_2}} \quad (5.1)$$

As the filter stage and therefore the roll-off slope increases, the low pass filters -3 dB corner frequency point and its pass band frequency changes from its original calculated value above by an amount determined by the following equation

$$f_{-3dB} = f_c\sqrt{2^{\frac{1}{n}} - 1} \quad (5.2)$$

The newly calculated cut-off frequency is $f_c = 10.243$ kHz. The new cut-off frequency still satisfy the 3 kHz requirement. The filter circuit is illustrated in figure 5.2.

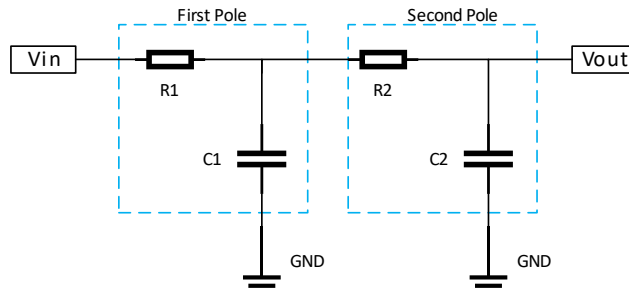


Figure 5.2: Filter Circuit

5.2.2. Amplifier

The amplification of the output from the Doppler sensor, needs to be both variable and stay within 1 V_{rms} swing. The best method of amplification is to make use of a differential amplifier. The differential op-amp gain equation is shown below

$$V_{\text{OUT}} = \frac{R3}{R2} \times (V_b - V_a) \quad (5.3)$$

The amplifier is illustrated in figure 5.3, resistor R3 will be a rheostat and R2's size is $1 \text{ k}\Omega$. Thus a variable resistor that ranges up to around $470 \text{ k}\Omega$ is used to allow for a gain of up to 470. Extracted from the datasheet of the op-amp, MCP602 [19], the gain versus frequency plot is illustrated in figure C.1. The gain settles at 60 dB, which equals a gain of 1000, then starts to fall off at 1 MHz. The expected frequency should range from 1 to 3000 Hz, so the gain specifications can be met with one op-amp.

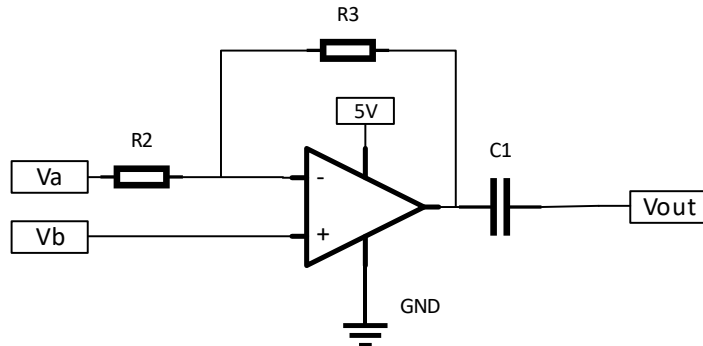
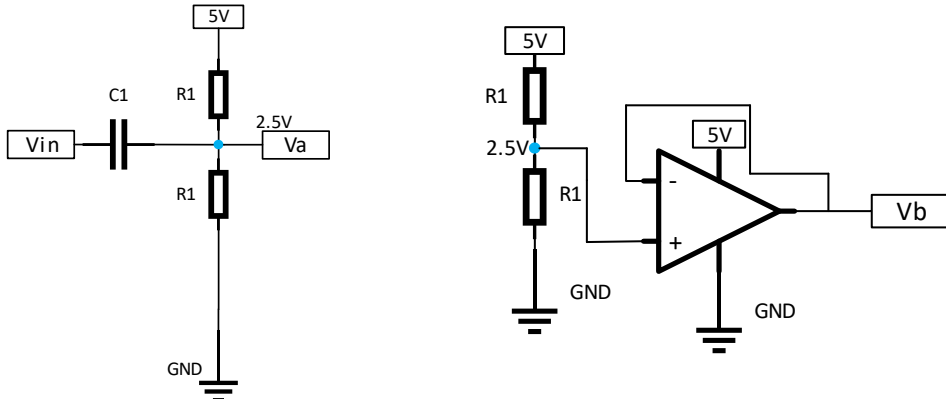


Figure 5.3: Amplifier Circuit

The voltage labels V_a and V_b , will both be centred around 2.5 V to give optimal swing on the output of the op-amp. The output will also swing around 2.5 V. The common mode input limits of the MCP602 op-amp ranges from $V_{ss}-0.3$ to $V_{DD}-1.2$, with $V_{ss}=0$ and $V_{DD}=5$, the limits ranges from -0.3 to 3.8 . Therefore 2.5 V safely lies between the common mode voltage limits. The circuit required to produce voltage V_a is illustrated in 5.4, a decoupling capacitor is placed between the output voltage from the filter and the 2.5 V DC voltage that the AC will swing around. The voltage node between the two resistors is calculated by the equation below

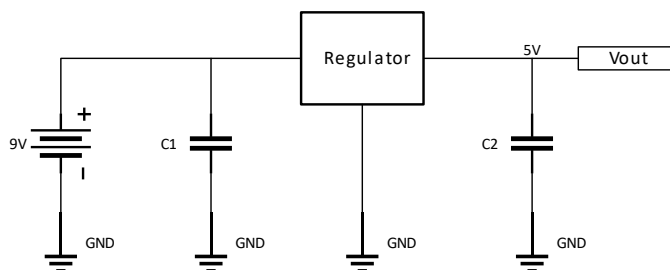
$$V_{\text{ref}} = 5 \times \frac{R1}{2 \times R1} = \frac{5}{2} \quad (5.4)$$

the value of R1 does not matter as long as the resistors are equal in size. The values are thus chosen to limit current and are $100 \text{ k}\Omega$. A voltage follower is added between V_{ref} and V_b reference to stabilize the 2.5 V as the output swings, illustrated in figure 5.5. Voltages V_a and V_b are attached to the same labels in the circuit illustrated in figure 5.3.

**Figure 5.4:** Voltage Swing Circuit**Figure 5.5:** Voltage Reference Circuit

5.2.3. Voltage Regulator

The regulator circuit for generating 5 V is illustrated in figure 5.6. Capacitor C_1 is placed to help with input stability and C_2 is placed to help with the transient response. It is important to use a low noise voltage regulator to limit noise in the circuit, therefore a LM7805 regulator is used [20]. The input voltage will be 9 V coming from an alkaline battery [21]. The expected output current will not exceed 200 mA. The power dissipated by the voltage regulator is 1 W and therefore there is no need for a heat sink or to do thermal calculations.

**Figure 5.6:** Voltage Regulator Circuit

5.2.4. Clipper

The clipper circuit is designed to limit the voltage swings at $\pm 1V$. This is achieved with a diode clipper circuit illustrated in figure 5.7. Two diodes are both placed with different polarity facing V_{in} , this will clip the voltage level at the forward voltage drop of the diodes. After testing different diodes the forward voltages were around 0.56 V. To satisfy the $1V_{rms}$ four diodes are needed in the circuit with two of them having the same polarity. This limits the voltage swings at $\pm 1.12V$ resulting in an RMS value of $0.79V_{rms}$. A decoupling capacitor is placed between the output of the clipper circuit and the ADC sampling point to further block any DC voltage.

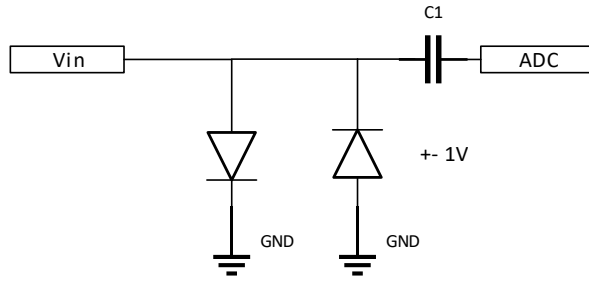


Figure 5.7: Diode Clipper Circuit

5.2.5. Antenna

To increase the range of the radar, a horn antenna is used to increase the gain G of the antenna. Noting equation 3.11, the range will increase relative to the gain increase of the order $G^{1/4}$. Together with the increased gain the horn antenna aims to focus the radiation pattern of the radar to a narrower beam.

The first part of a horn antenna is a waveguide. The waveguide act as a feed for the signal propagating from the patch antenna into the horn [22]. Figure 5.8 illustrates the shape of a rectangular waveguide. The main modes of propagation in the waveguide is either Transverse Electric Mode(TE mode) or Transverse Magnetic Mode(TM mode). There are infinite TE_{mn} modes, with $m \neq n$.

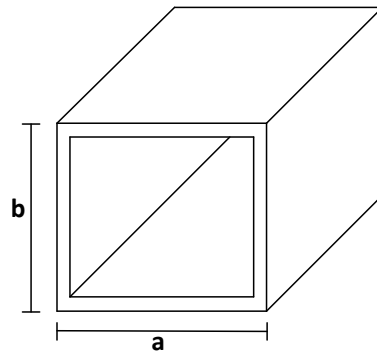


Figure 5.8: Rectangular Waveguide

The width a and height b parameters is used for designing the cut off frequency of the TE_{mn} mode in the waveguide. The equation for calculating the cut off frequency is shown below,

$$f_{cmn} = \frac{c}{2\pi} \sqrt{\left(\frac{m\pi}{a}\right)^2 + \left(\frac{n\pi}{b}\right)^2} \quad (5.5)$$

Considering TE_{10} mode as the dominate mode and $a \geq b$, the equation is simplified to

$$f_{c10} = \frac{c}{2a} \quad (5.6)$$

The micro strip lines, on the HB100 feeding the patch antenna, also transmits EM waves

and this causes the waveguide not to work if they are inside the rectangular waveguide. The lines also cause surface waves, illustrated in figure C.5, that affects the waveguide. The waveguide is therefore designed not to include the micro strip lines and where the waveguide is to be right above the micro strip line a cut out is made so that the surface waves does not affect it. The designed waveguide is shown in figure E.6 with a cut off frequency of 7.5 GHz.

Figure 5.9 illustrates the geometry of a horn antenna. W is the width of a rectangular aperture, and a is the radius of a circular aperture. The distance from the junction of the projected sides to the aperture is the slant radius R .

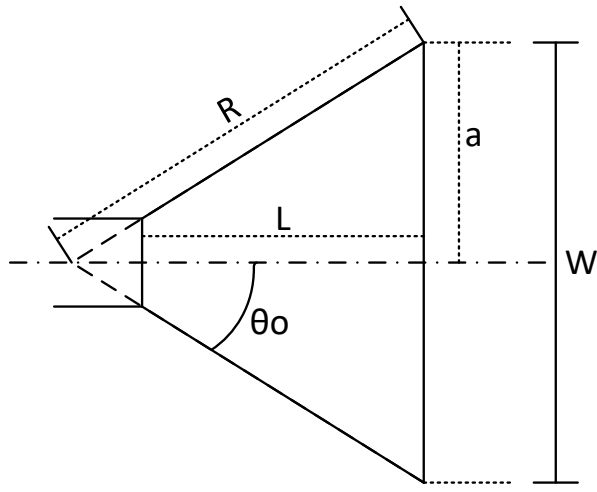


Figure 5.9: Horn Geometry

The dimensionless constant S [23] is represented by

$$S = \frac{W^2}{8\lambda R} = \frac{a^2}{2\lambda R} \quad (5.7)$$

Figure C.3 relates the relative field strength to the length of the horn antenna. The relative field strength graph is used to design the size of the sidelobes of the radiation pattern. Different models were designed in CST with taking into account what the manufacturing capabilities available. The final model is illustrated in figure E.1, with the radiation pattern is illustrated in figure E.2.

5.2.6. Software

The common signal processing technique used in radars is to determine the strongest frequency component in a short period, through an STFT [24]. This frequency component is then converted to speed. The speed algorithm 4.1 is designed on this basis. The algorithm takes as inputs the recorded file, sampling rate, frame size, overlap and size. The output of the file will be an array with the speeds measured from the strongest frequency component in that short period.

The flow diagram of the speed algorithm is illustrated below.,

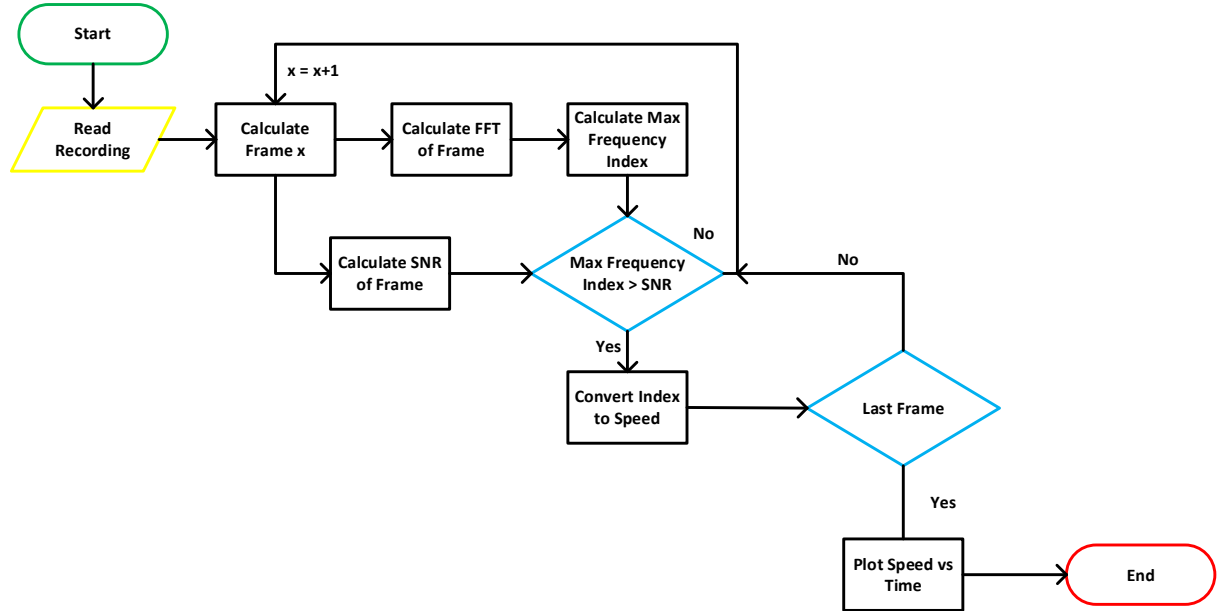


Figure 5.10: Speed Algorithm

The SNR level is calculated dynamically on each iteration of an STFT. This dynamically changes the level of the SNR, which leads to a better estimate of targets. This also improves the speed algorithms capability when the radar is placed in different measurement locations. This is also the standard calibration, to determine the SNR of the location, when a permanent radar is installed in the field. The SNR algorithm is illustrated in algorithm 4.2.

Algorithm 4.3 is the tracking of a vehicle algorithm. This entails establishing a vehicle and tracking its speed for as long as it is in range of the radar. The algorithm will assume only one vehicle will be in the range of the radar. The STFT time period is used to determine the assumed maximum change in speed a vehicle can exercise. This speed variation is then used to set up bin ranges in the frequency domain. When the following STFT is calculated and a target is identified within these limits the new target frequency is used to update the bin ranges. This process repeats until the target falls outside of the range of the bins, meaning the target is out of range or possibly not the same vehicle. The equation below relates the measured frequency to speed,

$$\text{Speed} = \frac{\text{Frequency}}{19.49} \quad (5.8)$$

Assume the fastest change in speed a vehicle can exercise in a second is 9 km/h. The change in time per frame can be calculated by the equation below,

$$time = (1 - overlap) \times \frac{length}{Fs} \quad (5.9)$$

with *overlap* being the percentage the frames overlap, *length* the size of the DFT and *Fs* the sampling frequency. The change in speed per second should be scaled as the size of the DFT frame changes, the relationship between DFT frame size and speed change is shown below,

$$(1 - overlap) \times \frac{length}{Fs} \times 9 = \frac{Frequency}{19.49} \quad (5.10)$$

Equation 5.11 relating the measured frequency to the index of the DFT. The DFT index is represented by *k*.

$$Frequency = \frac{k \times Fs}{length} \quad (5.11)$$

Substituting equation 5.11 into equation 5.10 and simplifying it, relates the DFT index to speed change. The bin range *k* for speed change is shown below,

$$k = \left(\frac{length}{Fs} \right)^2 \times 175.41 \quad (5.12)$$

The generation of the spectrogram is illustrated in algorithm 4.4. The algorithm requires the input parameters signal, filter type, overlap and frame size.

The cosine correction algorithm is illustrated in 4.5. The cosine correction is calculated by first determining the the maximum distance *R_{max}* that the vehicle was measured from the radar. The distance *d* is known and with the two distances the cosine angle can be calculated by equation 4.1. With the cosine angle β the corrected speed can be calculated with equation 4.2. The equation below is used to update the distance a vehicle is from the radar with each speed measurement.

$$R_{max} = R_{max} - \frac{length}{Fs} \times (1 - overlap) \times \frac{speed}{3.6} \quad (5.13)$$

Chapter 6

Results

6.1. Radar and Setup

Illustrated below is the structure and hardware of the radar. The radar is built on a wooden structure that imitates the size and height of a real speed radar.



Figure 6.1: Side View of Radar



Figure 6.2: Back View of Radar

The radar is placed next to a road located at 3 m from the center. The radar is pointed at the oncoming vehicles. The vehicle used for testing is a Nissan X-trail. Inside the car the GPS unit is placed that will also log the GPS data of the vehicle for speed comparison. The setup is illustrated below,

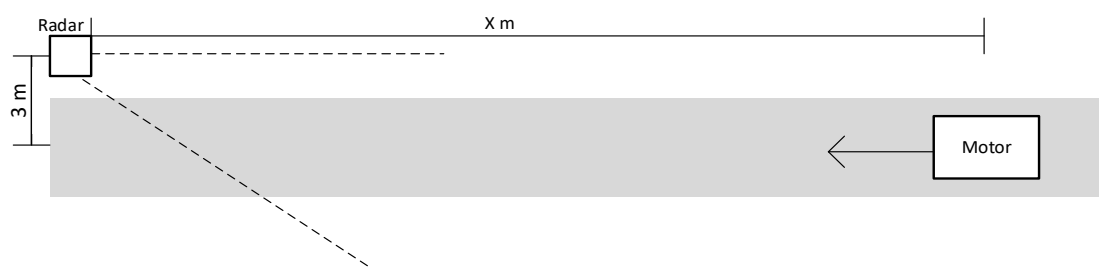


Figure 6.3: Radar Setup

6.2. Radar Results

The radar hardware designed in Chapter 5, was simulated in LTSpice and the radar software was simulated in Matlab. The circuits and results are illustrated in Appendix F.

To accurately test the radar, the measured speed of the radar is compared with the GPS speed measured from the Ublox GPS module. The spectrogram, illustrated in figure 6.4, clearly indicates the measured vehicle in a yellow line. The recording is imported into Matlab where the vehicles speed is measured. The radar speed is compared to the GPS speed in figure 6.5.

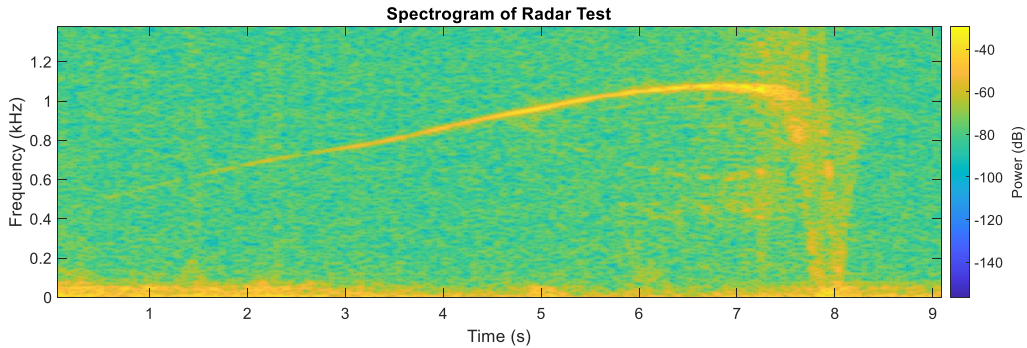


Figure 6.4: Measured Spectrogram of Vehicle

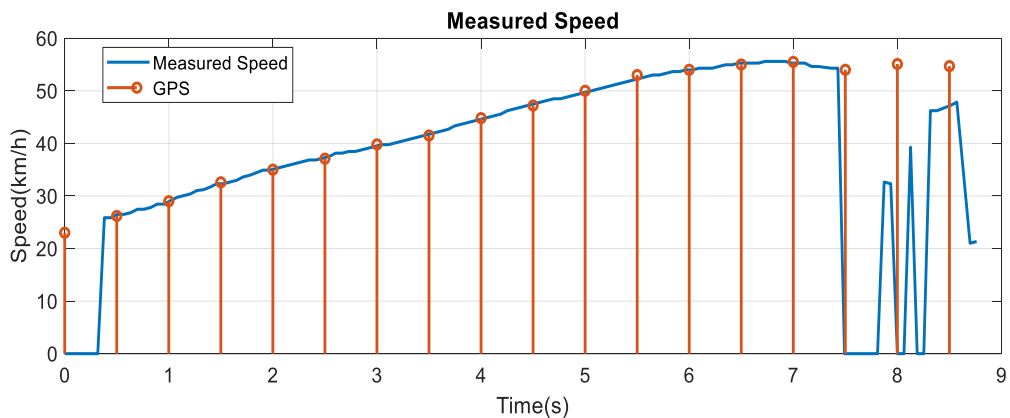


Figure 6.5: Speed Measured from Radar and GPS

The radar is capable of accurately measuring the speed of a vehicle and is similar to that of the GPS measurement. From this measurement the radars maximum range is calculated as $R = 85.7m$.

6.3. Results of Limitations

6.3.1. Results of Cosine Effect

Section 4.1 explains the cosine effect. As concluded in that section, the measured speed will always be less than the real speed of the vehicle. The measurement used to test the radar is taken as the original measurement. The cosine error is then corrected with offset of $d = 3m$ and $d = 6m$. By knowing the maximum distance from which a vehicle is visible to the radar. Software can be used to estimate and correct the cosine error. The corrected cosine error for both distances d are illustrated in the figure 6.6. Note that when the vehicle is within 3 to 5 m of the radar, the speed of the vehicle is no longer measurable due to saturation. Consequently the cosine error gives false corrections. This phenomenon is discussed in section 6.3.6.

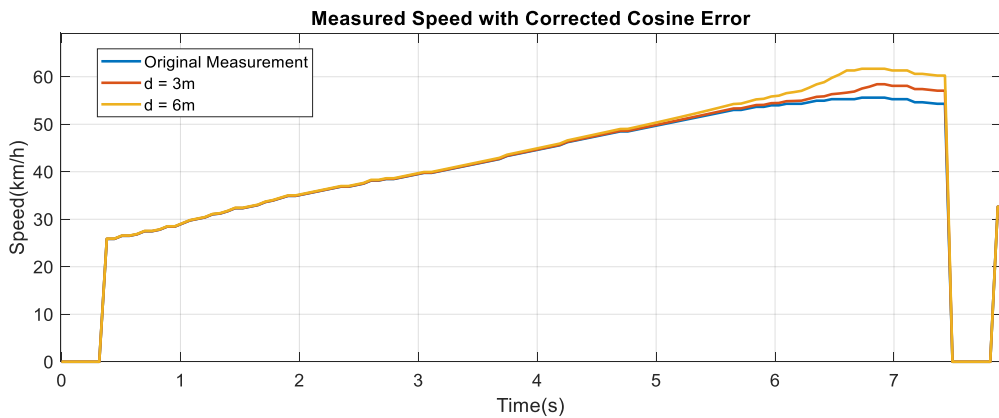


Figure 6.6: Cosine Error on Vehicle Speed

Despite being able to correct the cosine error. The operation and setup of a radar is very important. The radar is not capable of determining in what lane the vehicle will be travelling. This means that the radar cannot correct the cosine error on more than one lane at a time. The cosine error can only be corrected where the distance d will remain the same for all vehicles passing by the radar. Multiple lane application will result in erroneous measurements. When the vehicle is limited to traveling in one lane at a fixed distance d , the cosine error might be small enough for most of the distance it is measured, that no correction is needed. For the speed measurement illustrated in figure 6.6, the cosine error is only visible once the vehicle is within 10 to 20m of the radar.

6.3.2. Results of Accuracy and Acceleration Limits

The configuration of the DFT sample size is important for the accuracy of a radar as mentioned in Section 4.2. To illustrate this phenomenon a vehicle accelerating past the radar is measured. The radar accurately calculates the acceleration of the vehicle without

too many calculations. The accompanying spectrogram with the best combination of time and frequency is shown in figure G.1 and the speed measurement is shown below,

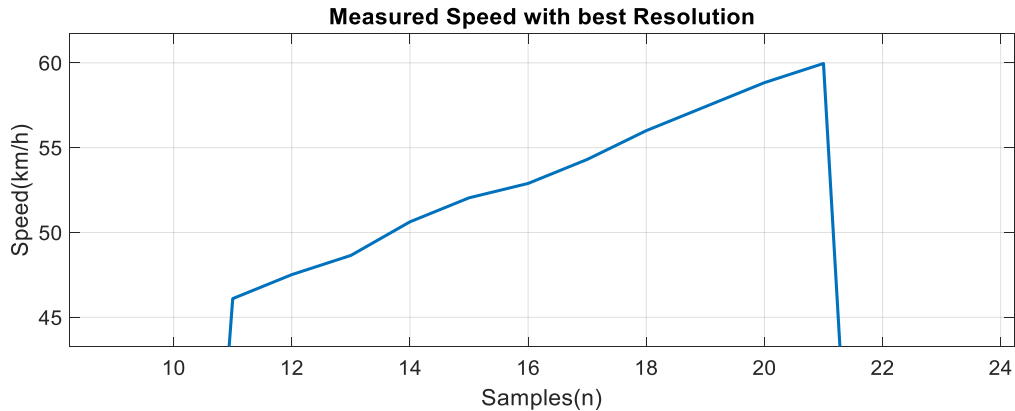


Figure 6.7: Measured Speed with best combination of Time and Frequency Resolution

When the DFT sample size is too big. The radar is incapable of calculating a fast change in speed. This is illustrated in figure 6.8. The measured speed is not an accurate estimate of the accelerating vehicle. The change in speed per sample is around 3.5 km/h which does not satisfy the required accuracy for a radar. The accompanying spectrogram, illustrated in figure G.2, clearly indicates how the radar is capable of differentiating between frequency components, but unable to differentiate in time.

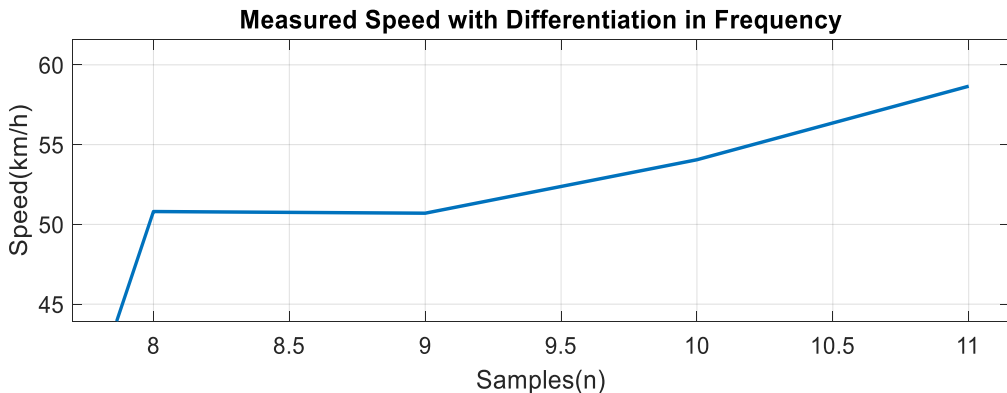


Figure 6.8: Measured Speed with Differentiation in Frequency

If the DFT sample size is too small. The radar is measuring the acceleration accurately but there are an excessive amount of measurements. This will require powerful processing which is unnecessary. Some of the measurements recorded the same speed as the previous measurement. In comparison to figure 6.7, which requires 10 samples, figure 6.9 calculates 25 samples. The accompanying spectrogram is shown in figure G.3. The spectrogram is a clear indication of how the frequency differentiation is lost when time differentiation is prioritised.

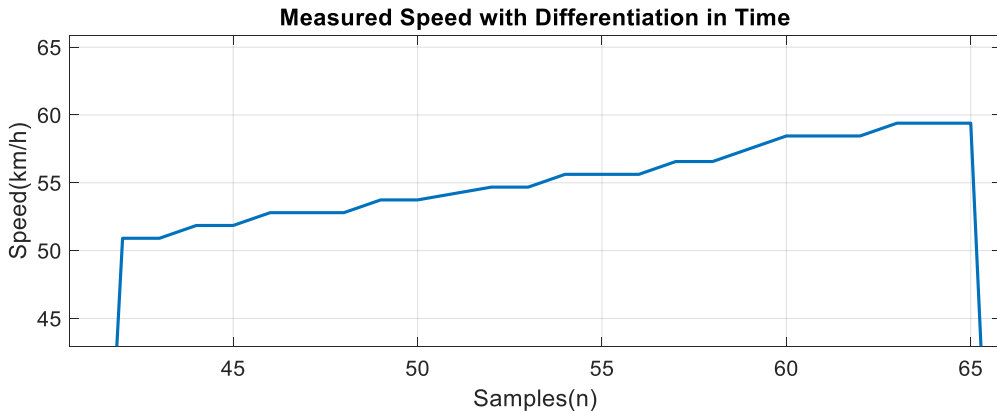


Figure 6.9: Measured Speed with Differentiation in Time

The table below concludes the differences between sampling sizes. As the sample size decreases the acceleration accuracy increases and vice versa.

Table 6.1: Comparison between Sample Sizes

	Best Resolution	Time Resolution	Frequency Resolution
Frame Size(s)	0.1224	0.0289	0.5442
Acceleration(km/h)	1.4	0.33	3.5

6.3.3. Results of Object Identification

To illustrate the effect of a vehicles RCS, the maximum measurable distance is compared to each other. The bigger the RCS the further the vehicle will be picked up by the radar. The spectrogram of the large vehicle is shown below and the maximum measurable distance is 65m. In comparison the spectrogram of the motorcycle is illustrated in figure 6.11, where the maximum measurable distance is merely 37m. Equation 3.15 relates the large vehicles RCS to be 9.5 times that of the motorcycle's RCS.

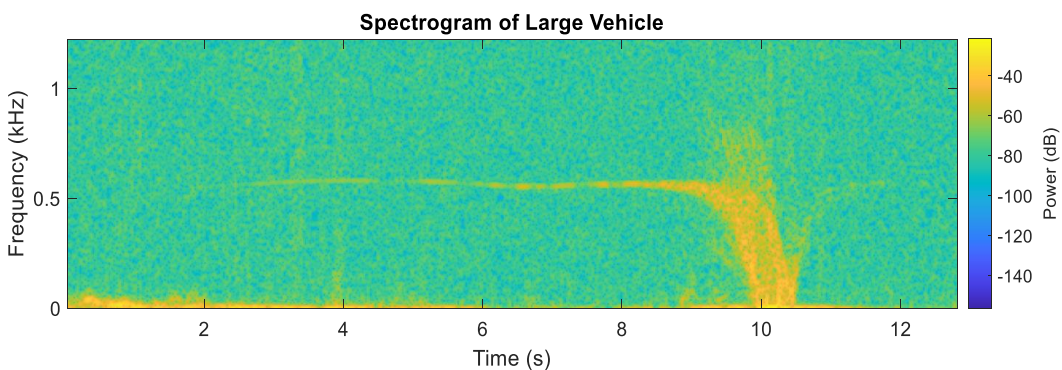


Figure 6.10: Spectrogram of Large Vehicle

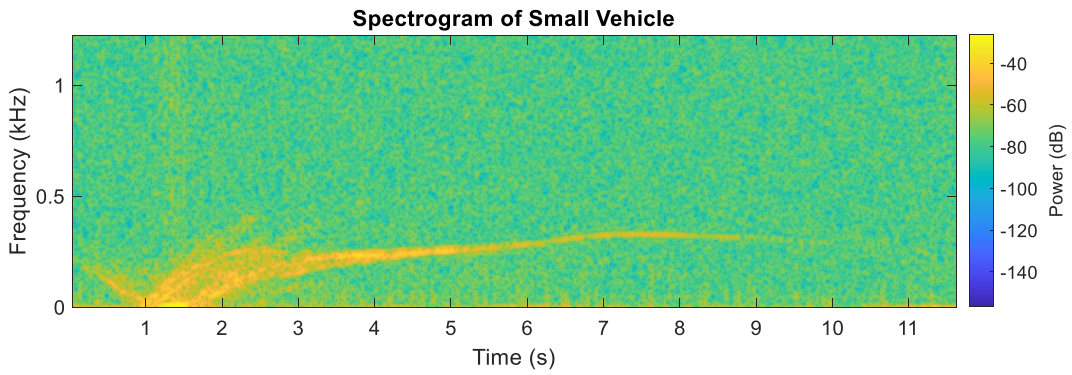


Figure 6.11: Spectrogram of Small Vehicle

The radar is unable to determine which direction a vehicle is travelling. The radar is also unable to assign a signal to a vehicle if more than one vehicle is present. This ultimately leads to the radar only being able to track one vehicle. The spectrogram below shows two vehicles being measured. The measured speed is shown in figure 6.13. The speed graph shows only one tracked vehicle.

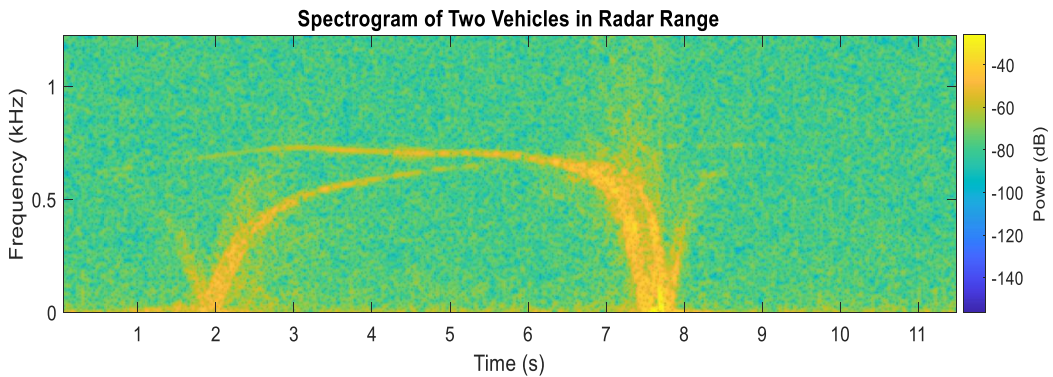


Figure 6.12: Spectrogram of Two vehicles in Radar Range

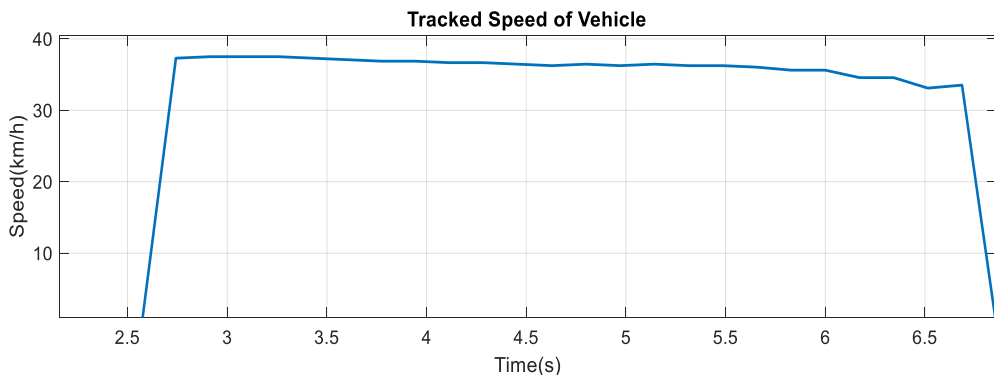


Figure 6.13: Tracked Speed of Vehicle

6.3.4. Results of Antenna Sidelobes

To demonstrate the effect of antenna sidelobes, the radar will be rotated from north to illustrate the importance radiation pattern and radar setup can have on the measurements. Table 7.1 indicates the radars measurable range before and after adding the horn antenna. As the radar is rotated the HB100 sensor still has good range while the Horn antenna which has a more directed radiation pattern loses most of its ability to measure a vehicle. Figure 6.14 illustrates how radiation patterns of the HB100 sensor and horn antenna differs.

Table 6.2: Measurable Distance of Radar

Degrees West of North	HB100 Antenna	Horn Antenna
0°	62m	85.7m
30°	52m	32m
60°	30m	21m

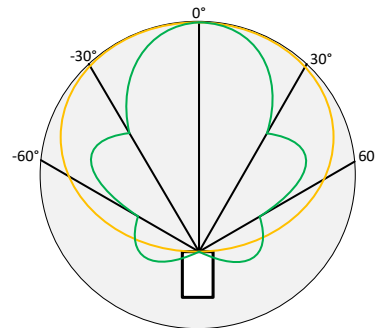


Figure 6.14: Comparison of Radiation Patterns between HB100 and Horn Antenna

6.3.5. Results of Multiple Path Reflection

To demonstrate the multiple path reflection effect a metal surface was created by covering a piece of wood with foil. The self made "billboard" is illustrated in Figure C.4. The multiple path reflection setup is illustrated below, the red lines indicates the radar is measuring the reflection from the "billboard". The blue line shows when the radar measures the vehicle and then the blue striped line is to indicate when the radar is incapable of measuring the vehicle.

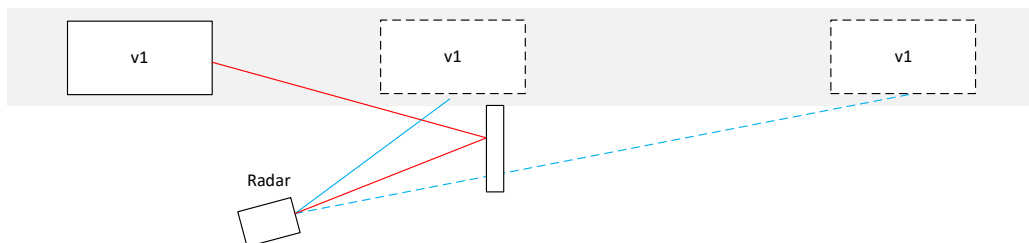


Figure 6.15: Multiple Path Reflection Setup

The measured spectrogram is illustrated in Figure 6.16. It indicates the vehicle is measured while it is still traveling behind the radar. The vehicle then passes by the radar, where saturation occurs and then the vehicle passes behind the "billboard", where the radar does not detect the vehicle. Once the vehicle is far enough away from the radar. The radar is then able to measure the vehicle again.

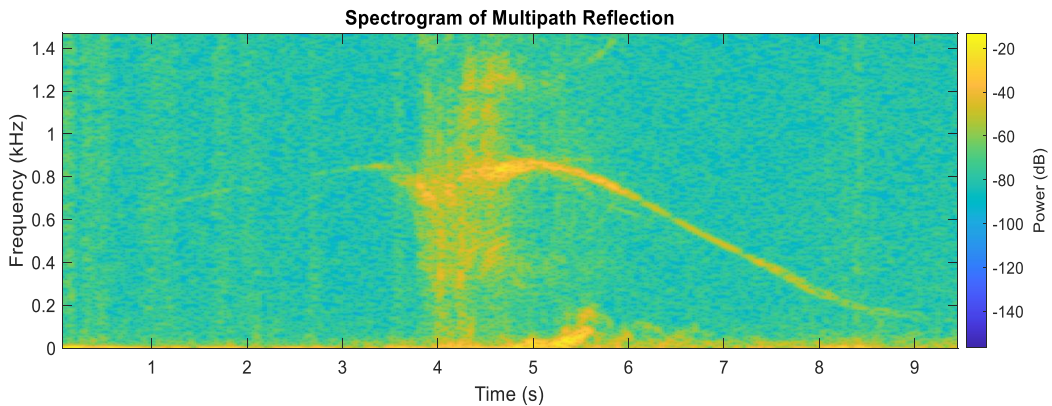


Figure 6.16: Spectrogram of Multiple Path Reflection

The radars tracking ability is shown in figure 6.17. It is clear that the radar is capable of tracking the vehicles reflection from the "billboard". It also illustrates when the vehicle has passed the "billboard" and is tracked again.

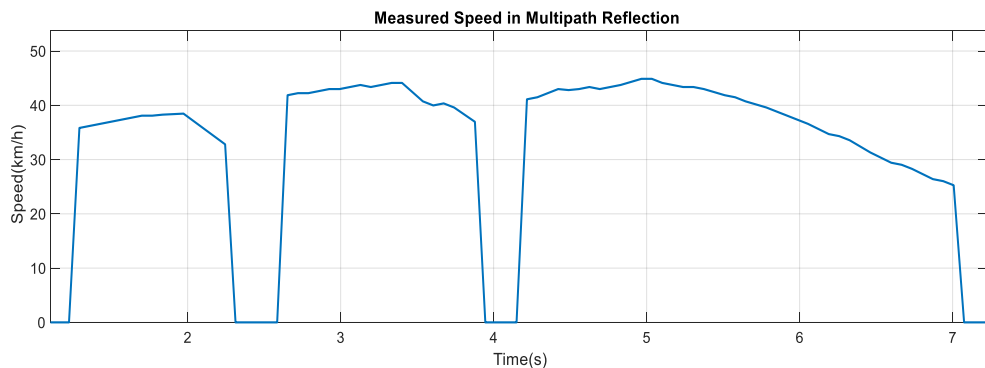


Figure 6.17: Tracked Speed of Multiple Path Reflection

6.3.6. Results of Radar Receiver Saturation

As discussed in Section 4.6, the radar is subject to saturation whenever a vehicle drives closely by the radar. This will cause a moment where the radar will be blind to any moving vehicles in the range. Depending on how the radar is set up. If vehicles are coming from the opposite direction the radar is pointing in. The radar to unexpectedly lose its visibility. Figure 6.18 illustrates the spectrogram of two vehicles, one moving towards the radar from the direction it is pointing in and one vehicle moving in the opposite direction. The saturation causes the radar to lose its tracking of the first vehicle for a moment. The

radar is then locked on to the second vehicle until the first vehicle passes by the radar and the phenomenon occurs again.

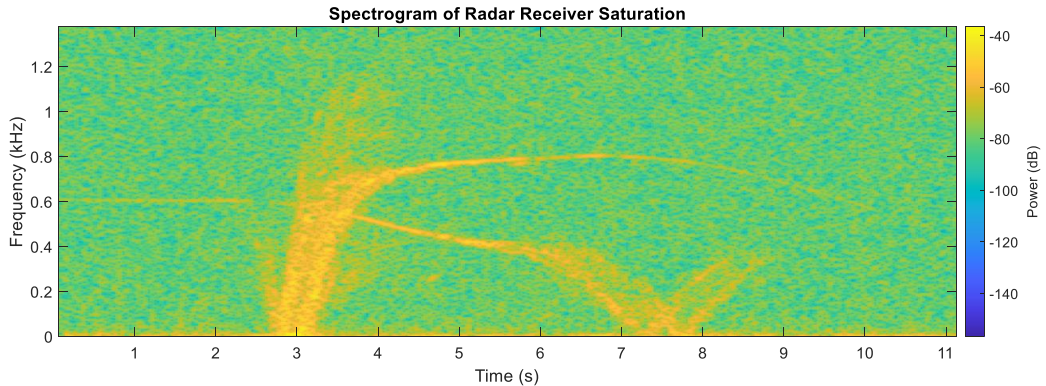


Figure 6.18: Spectrogram of Radar Receiver Saturation

The tracking software applied is and illustrated in figure 6.19. The graph clearly illustrates when there is a vehicle passing by the radar and where the radar is and is not capable of tracking a vehicle.

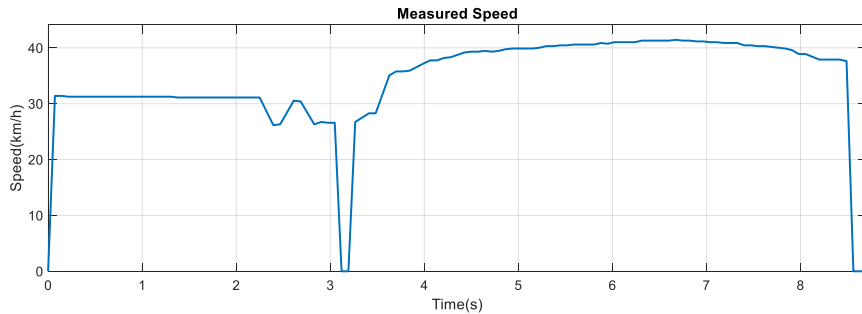


Figure 6.19: Speed tracking when Saturation occurs

An extreme case of receiver saturation is illustrated in figure 6.20. The second and third harmonics are clearly visible from the measurement and this is due to the saturation of the mixer.

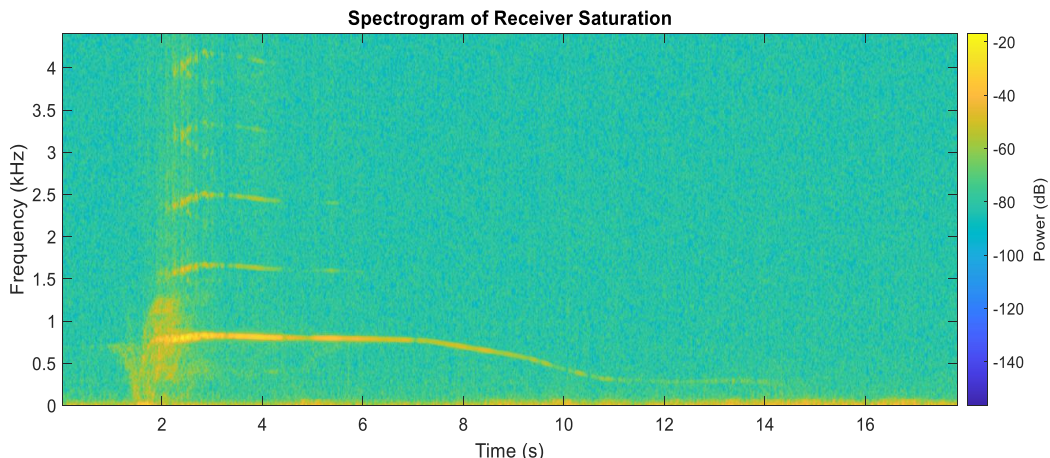


Figure 6.20: Extreme Receiver Saturation

Chapter 7

Conclusion

7.1. Objectives

Below are the responses to what degree each objective was achieved.

Table 7.1: Response to Objectives

Objectives	Response
1. Identify the possible limitations of CW Doppler radars in vehicle speed measurements	After a thorough literature study, the six limitations of a CW Doppler radar in vehicle speed measurements were identified
2. Develop hardware for a CW Doppler radar that can perform up to 80 m	The CW Doppler radar is capable of measuring vehicles up to 85m, subjective to a vehicle RCS. The biggest car was a Nissan X-trail if for instance a truck was used it would have been measured from further away
3. Develop software capable of calculating the speed of targets	The developed software is capable of accurately measuring a vehicle's speed. It was compared to GPS speed data
4. Develop software capable of tracking a vehicle	The developed software is capable of tracking a vehicle in the measurable range of the radar
5. The radar should be able to distinguish between a vehicle and clutter	The radar is capable of clearly distinguishing between a vehicle and clutter
6. Test the theorized limitations of CW Doppler limitations in vehicle speed measurements	All the limitations were tested and their results were illustrated in Section 6.2
7. Determine whether the laws and regulations are satisfactory in limiting possible errors and limitations	The conclusion is discussed in Section 7.2

7.2. Operations

To determine whether the laws are sufficient in limiting the limitations, the operation laws are related to the built radars specifications.

- No metal road signs or vertical flat surfaces larger than 1 meter in vertical height within 15° on either side of the aiming direction, within a distance of **30 meters** of the antenna.
- No signals received and processed from vehicles more than **70 meters** away
- No other moving vehicle other than the measured vehicle within **85 metres** from the radar in the direction of operation
- The vehicle's speed should be tracked for **0.5s** for a valid reading to be possible

The operation laws limit the use cases of a CW Doppler radar to only measure one vehicle at a time. The first limitation that is accounted for is the effect of multiple path reflection 4.5. The law specifies that no flat surface should be in the direction of the intended measurement. The next two laws state that only one vehicle should be measured for a measurement to be valid. The law however does not consider the difference in a vehicle's RCS size. The results of different RCS sizes are illustrate in Section 6.3.3. A CW Doppler radar cannot determine the RCS of a vehicle. Therefore this limitation cannot be corrected with laws. The last law states that a vehicle is required to be tracked before a measurement is accurate. The tracking of a vehicle does not deter any of the limitations as a vehicle can be tracked even if it is not the only vehicle in the range of the radar. Figure 6.12 illustrates the phenomenon where two vehicles are travelling at the same speed and are thus tracked as one vehicle. The laws make no notice of the cosine effect 4.1, receiver saturation 4.6 or the accuracy and acceleration limits 4.2. These limitations are mostly constricted to the radar designed and they should be addressed before being certified for use. The antenna sidelobes 4.4 are not considered but the limitation can be eliminated with a very directive antenna. This however limits the use of the radar to only one lane.

A CW Doppler radar can accurately measure a vehicle's speed. The accuracy of the measurement is limited to only one vehicle travelling in a single lane. After the investigation into the limitations of a CW Doppler radar, it is clear stricter operation laws are required.

7.3. Future Work

Possible future work can be a limitation study on an FMCW Doppler radar and its limitations to vehicle measurement and enforcement. FMCW Doppler radars have the added capability of range resolution. The FMCW Doppler radar can then be compared to the limitations identified in this report. FMCW Doppler radars are also popular in vehicle measurement and it would be significant to see how an FMCW Doppler radar solves the limitations of a CW Doppler radar.

Bibliography

- [1] Sutori, “The doppler effect.” [Online]. Available: <https://www.sutori.com/en/item/untitled-420a-4b20>
- [2] , “The catalina preservation society.” [Online]. Available: <https://pbycatalina.com/specifications/>
- [3] B. van der Riet, “An investigation of the integrity of the doppler radar measurement of vehicle speeds, with particular reference to the digidar 1-k instrument.”
- [4] ArriveAlive, “Prosecuting guidelines for speed measurement.” [Online]. Available: <https://www.arrivealive.co.za/Prosecuting-Guidelines-for-Speed-Measuring-Equipment>
- [5] N. C. Martin, “A microwave doppler technique for vehicle speed determination,” Masters Thesis, University of Cape Town, Rondebosch, Cape Town, 7700, 1987.
- [6] N. G. Lam, “Vehicle speed measurement using doppler effect,” Honours Thesis, VAASAN AMMATTIKORKEAKOULU UNIVERSITY OF APPLIED SCIENCES, Wolffintie 30, 65200 Vaasa, Finland, 2021.
- [7] *X-Band Microwave Motion Sensor Module Application Note*, ST Electronics, May 2018, rev. 1.
- [8] M. I. Skolnik, *INTRODUCTION TO RADAR SYSTEMS*. McGraw-Hill Book Co., 1981.
- [9] S. Farahani, “Rf propagation, antennas, and regulatory requirements,” *ZigBee Wireless Networks and Transceivers*, pp. 177–206, 2008.
- [10] I. T. Union, “Itu telecommunication standardization sector.” [Online]. Available: <https://www.itu.int/en/Pages/default.aspx>
- [11] K. S. INC., “Frequency information: K, ka, ku x bands.” [Online]. Available: <https://kustomsignals.com/blog/police-speed-radar-gun-frequency-information-k-ka-ku-x-bands>
- [12] A. E. Fuhs, “Radar cross section lectures,” Lectures, Monterey, California, Naval Postgraduate School, 411 Dyer Road, 1982.

- [13] P. R. I. Center, “Vehicle reflection.” [Online]. Available: <https://copradar.com/chapts/chapt3/ch3d6.htmls>
- [14] W. A. H. MARK A. Richards, James A. Scheer, *Principle of Modern Radar*. SciTech Publishing, 2010.
- [15] C. Wolff, “Radar basics.” [Online]. Available: <https://www.radartutorial.eu/01.basics/lrb02.en.html>
- [16] J. Beale, “Playing with cheap hb100 doppler radar module for car speed.” [Online]. Available: <https://www.eevblog.com/forum/projects/playing-with-cheap-hb100-doppler-radar-module-for-car-speed/>
- [17] “Audacity.” [Online]. Available: <https://www.audacityteam.org/>
- [18] *NEO-M8 u-blox M8 concurrent GNSS modules*, Ubxlo, Oct. 2021, rev. 1.
- [19] *2.7V to 6.0V Single Supply CMOS Op Amps*, Microchip, Oct. 2007, rev. 1.
- [20] *μ A7800 SERIES POSITIVE-VOLTAGE REGULATORS*, Texas Instruments, May 1976, rev. 1.
- [21] *12V Alkaline Battery*, RS PRO, Oct. 2022, rev. 1.
- [22] S. Rein, “Waveguide primer.” [Online]. Available: <https://www.microwaves101.com/encyclopedias/waveguide-primer>
- [23] T. A. Milligan, *Modern Antenna Design*. John Wiley Sons, 2005.
- [24] B. R. MAHAFZA, *Radar Systems Analysis and Design using Matlab*. CRC Press, 2013.

Appendix A

Project Planning Schedule

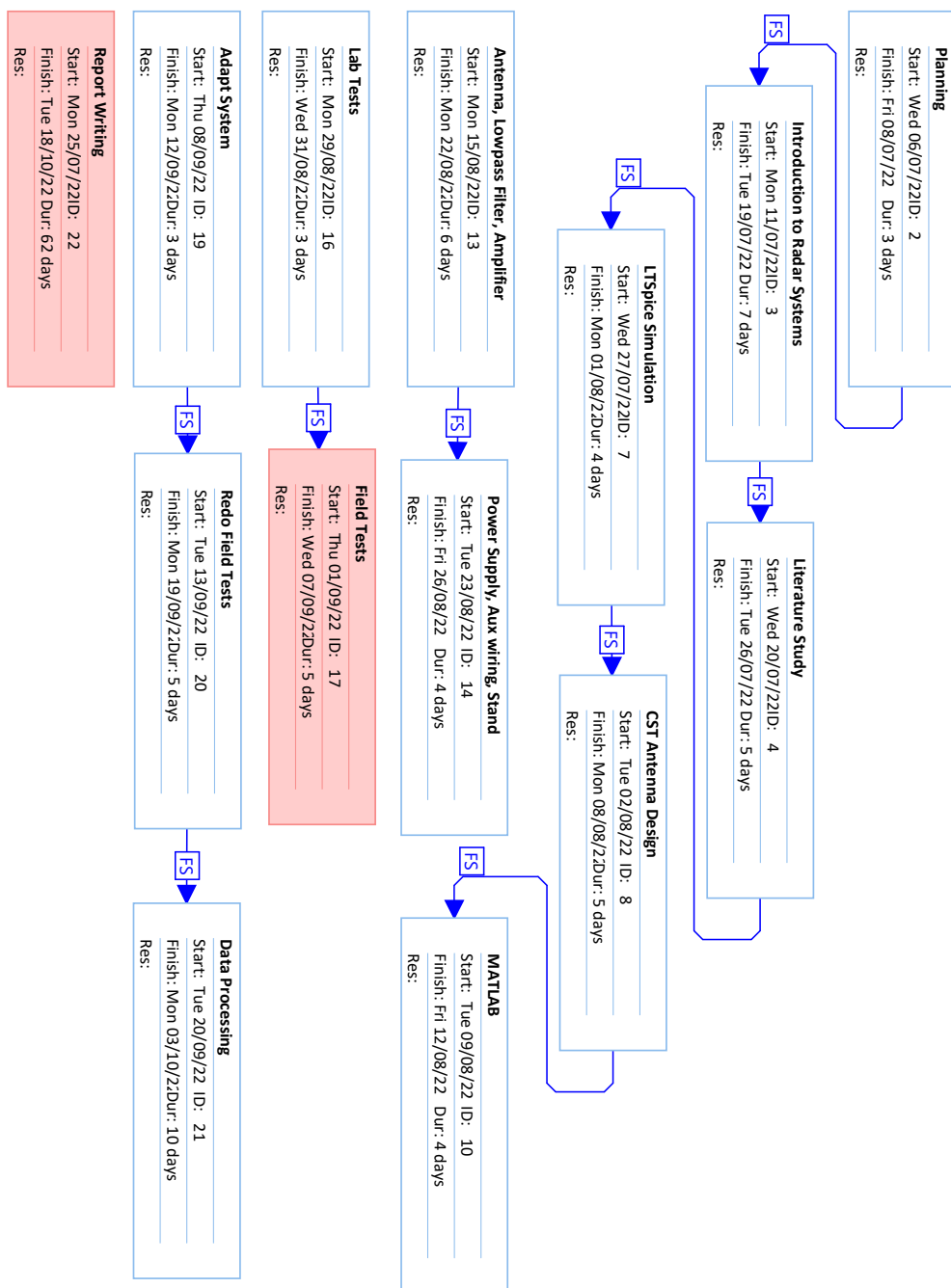


Figure A.1: Tracking Gantt Chart used for Project Planning

Appendix B

Outcomes Compliance

GA 1. Problem Solving: Identify, formulate, analyse and solve complex engineering problems creatively and innovatively.

The problem, "What are the limitations of a CW Doppler Radar", was under-specified and required intensive literature study on radars. It contained three sub-problems, formulation of the limitations of a CW Doppler Radar, building a Radar and testing the radar and its limitations. The solution required information from a wide variety of sources and is complex and also required originality.

GA 2. Application of Scientific and Engineering knowledge: Apply knowledge of mathematics, natural sciences, engineering fundamentals and an engineering speciality to solve complex engineering problems.

The scientific and engineering knowledge that I required and acquired to solve the problem ranged from electromagnetics, signal processing, electronic design and applied mathematics. For electromagnetics, I attained knowledge of wave propagation, waveguides and antenna theory. Signal processing is mainly applied to radar processing techniques like speed extraction and vehicle tracking. The electronic design was used in designing the radar hardware and conditioning the signals accordingly. Then applied mathematics relates to the combining of all of the above in a working radar and formulating the limitations.

GA 3. Engineering Design: Perform creative, procedural and non-procedural design and synthesis of components, systems, engineering works, products or processes.

I successfully applied engineering design to three domains. The first is to design a radar that consists of modules, electronic components and antennas. The second engineering design was to design software capable of performing the necessary task of a Doppler radar and to be able to illustrate the limitations. The last engineering design was in the form of tests, that would prove the radar is performing accurate and test the theorized limitations.

GA 4. Investigations, experiments and data analysis: Demonstrate competence to design and conduct investigations and experiments.

My first step in investigating the problem was to do a literature study on radars and specifically CW Doppler Radars. As I progressed with the project I also had to investigate radar software techniques and radar limitations. The experiments were exercised across multiple software and lab tools. For instance, I tested my hardware in both LTSpice and with lab tools, like an oscilloscope and signal generator. Matlab was used to experiment with software techniques, where I simulated a radar signal to test my software. CST was used to test and experiment with antenna designs. Data analysis was done in Matlab, where I made use of a combination of generated graphs and spectrograms.

GA 5. Engineering methods, skills and tools, including Information Technology: Demonstrate competence to use appropriate engineering methods, skills and tools, including those based on information technology.

A combination of engineering tools, like LTSpice, Matlab and CST were used. LTSpice was used for electronic circuit design. Matlab was used for software design, testing and data analysis. CST was used in antenna design and experimentation. Python was used for extracting GPS speed from NMEA data, which was acquired from a Ublox GPS module. Version control was done through GitHub and lastly, the report was constructed in Latex.

GA 6. Professional and technical communication. Demonstrate competence to communicate effectively, both orally and in writing, with engineering audiences and the community at large.

The project includes a written report and an oral presentation. These demonstrate competence to communicate effectively, both orally and in writing.

GA 8. Individual work: Demonstrate competence to work effectively as an individual.

I took primary responsibility for successful completion of all aspects of the projects.

GA 9. Independent Learning Ability: Demonstrate competence to engage in independent learning through well-developed learning skills.

I completed an MIT Lincoln Laboratory, a course on Radar Systems that formed a basis for my knowledge of radars. I then studied complementary work, consisting of articles, an honours thesis and two master theses. The bulk of the information I learned came from textbooks, namely Introduction to Radar Systems, by Merrill L. Skolnik and Modern Antenna Design by Thomas A. Milligan.

Appendix C

Figures

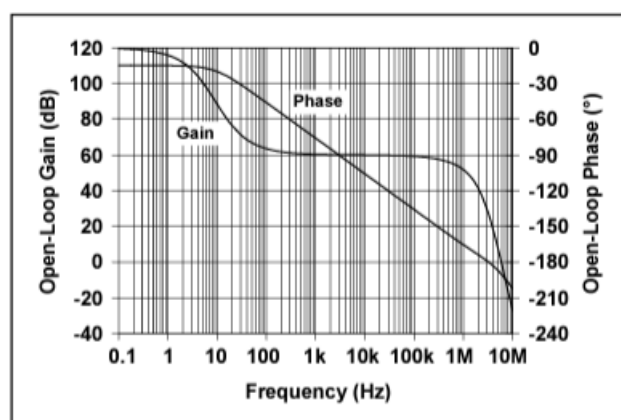


Figure C.1: Gain versus Frequency plot of MCP602 op-amp



Figure C.2: Ublox GPS Module

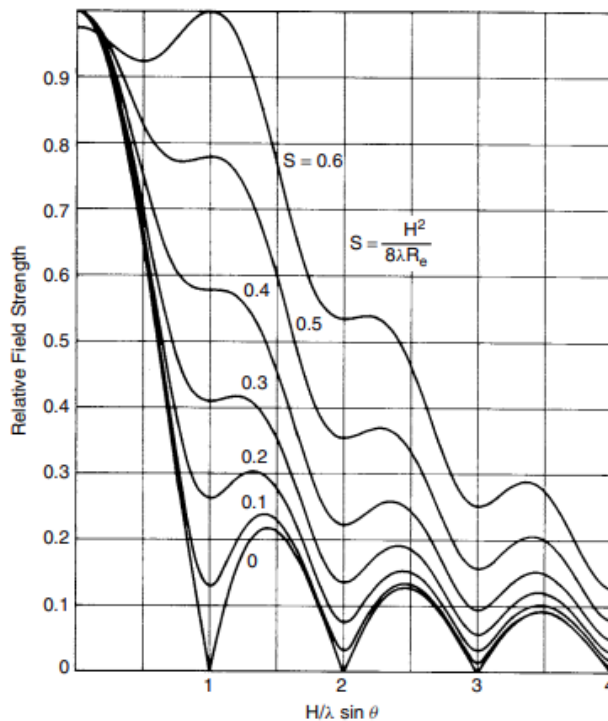


Figure C.3: Relative Field Strength Graph



Figure C.4: Homemade Billboard

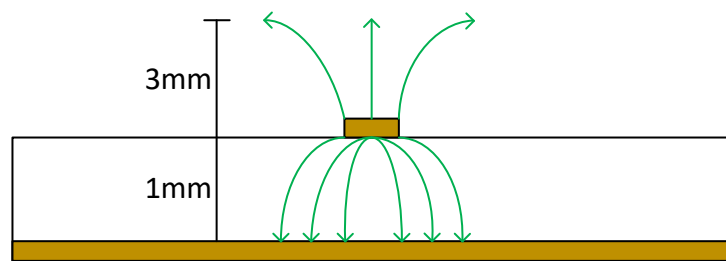


Figure C.5: Surface waves on micro strip copper line

Appendix D

Radar Software

Algorithm 4.1: Speed

input Recording, Sampling Rate, Frame Size, Signal-to-Noise Ratio
for $n = 0$ to $frames$ **do**
 Calculate FFT of sample
 Calculate maximum frequency component
 Store frequency component in array
for $n = 0$ to $frames$ **do**
 Convert frequency component to speed
 Plot speed versus time

Algorithm 4.2: Signal to Noise Ratio

input Recording, Sampling Rate, Frame Size
for $n = 0$ to $frames$ **do**
 Calculate FFT of Sample
for $i = 0$ to $SampleSize$ **do**
 Summation of Frequency Components
 Store SNR per frame
SNR = Summation of SNR per frame divided by total frames
output Signal-to-Noise Ratio

Algorithm 4.3: Tracking

input Recording, Sampling Rate, Frame Size, Frequency Bin Size, Speed Limit

for $n = 0$ to $frames$ **do**

- Calculate FFT of Sample
- for** $i = 0$ to $SampleSize$ **do**

 - Calculate Maximum Component
 - Calculate SNR
 - Convert Frequency to Speed
 - if** Speed > Speed Limit **then**

 - if** Maximum Component \geq SNR **then**
 - if** Frequency Difference \leq Bin Range **then**

 - Store Speed
 - Update bin range

Store Object Frequency

Plot Tracked Vehicle Speed vs Time

output Tracked Vehicle Speed

Algorithm 4.4: Spectrogram

input Signal, Sampling Rate, Frame Size, Filter Type, Overlap

Generate Spectrogram

output Spectrogram

Algorithm 4.5: Cosine Angle Correction

input Measured Speed, Maximum Measured Distance, d

for $n = 0$ to $frames$ **do**

- Calculate change in Distance
- if** $d \geq 5$ **then**

 - Calculate Cosine Angle
 - Calculate Corrected Speed

Plot Corrected Speed vs Time

output Corrected Speed

Appendix E

Antennas

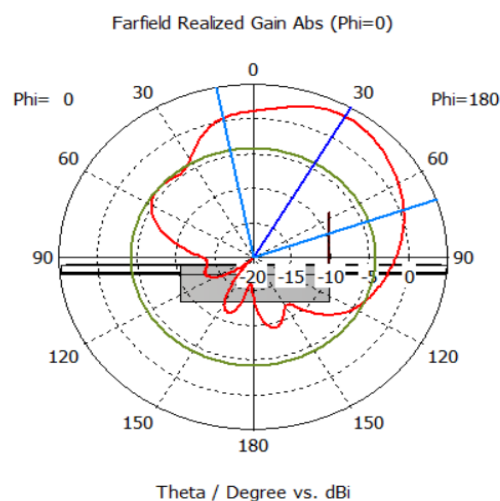


Figure E.1: HB100 Radiation Pattern in CST

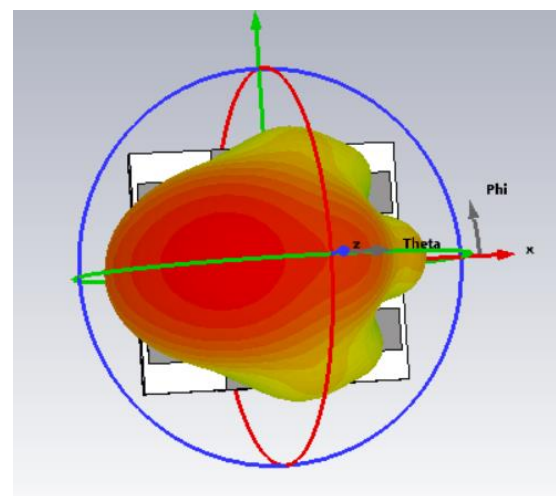


Figure E.2: HB100 3D Radiation Pattern in CST

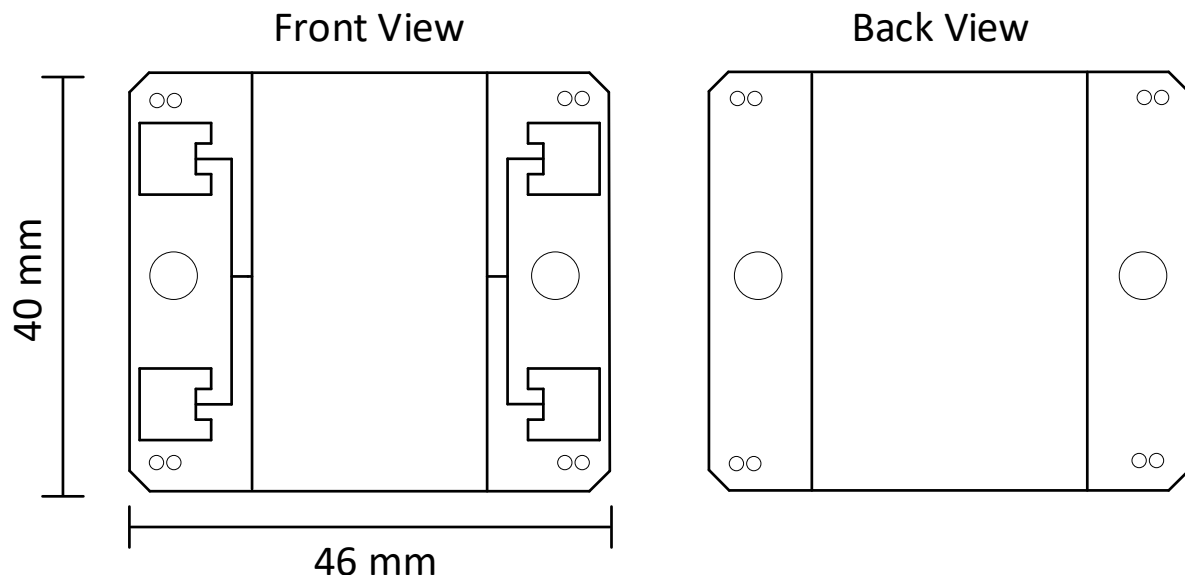


Figure E.3: Schematic Drawing of HB100 Sensor

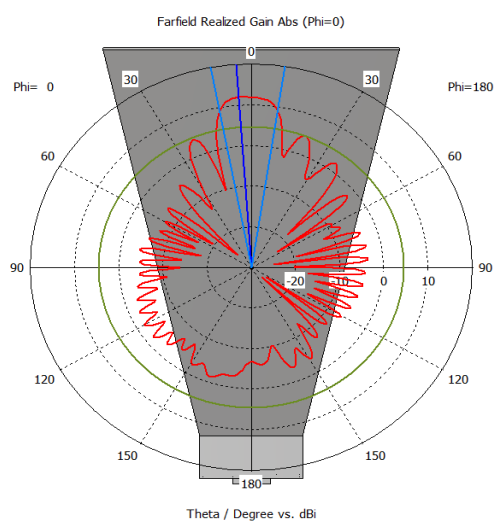


Figure E.4: Horn Antenna 1D Radiation Pattern

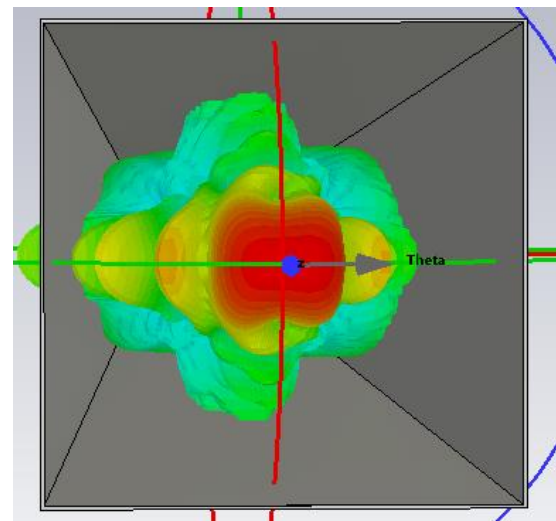


Figure E.5: Horn Antenna 3D Radiation Pattern

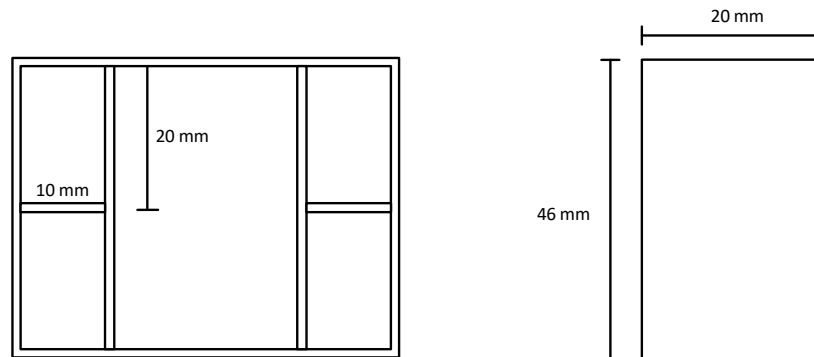


Figure E.6: Schematic Drawing of Waveguide

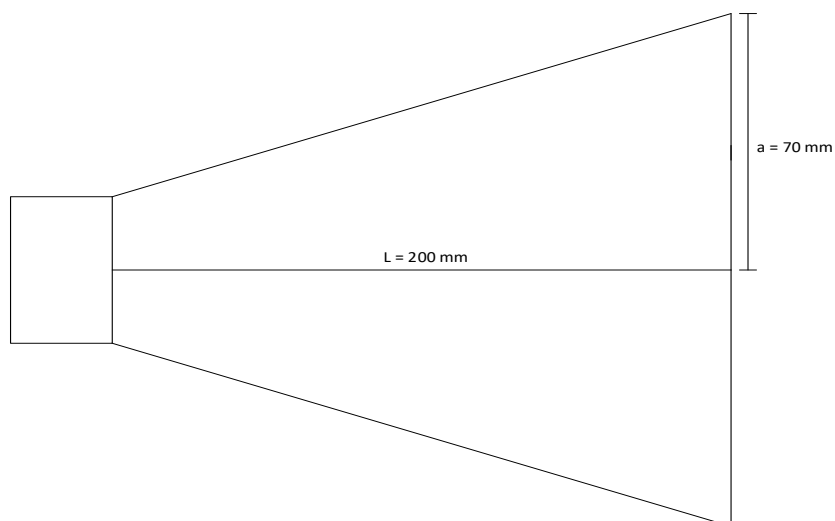


Figure E.7: Schematic Drawing of Horn Antenna

Appendix F

Radar Simulations

The appendix details the simulation of the radar hardware in LTSpice. Figure F.1, demonstrates the workings of the amplifier and lowpass filter. Figure F.2, demonstrates the frequency response of the filter. The whole circuit is illustrated in figure F.3.

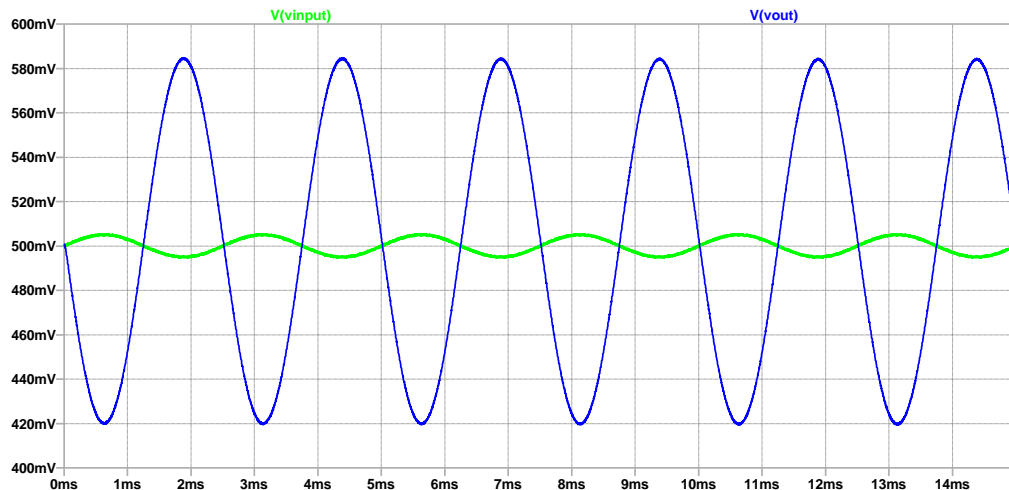


Figure F.1: Input and Amplified Output

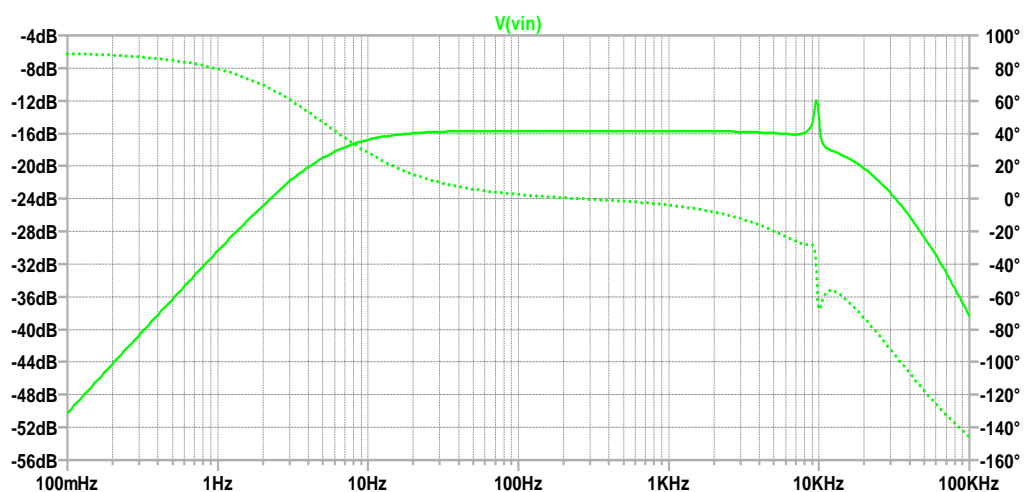
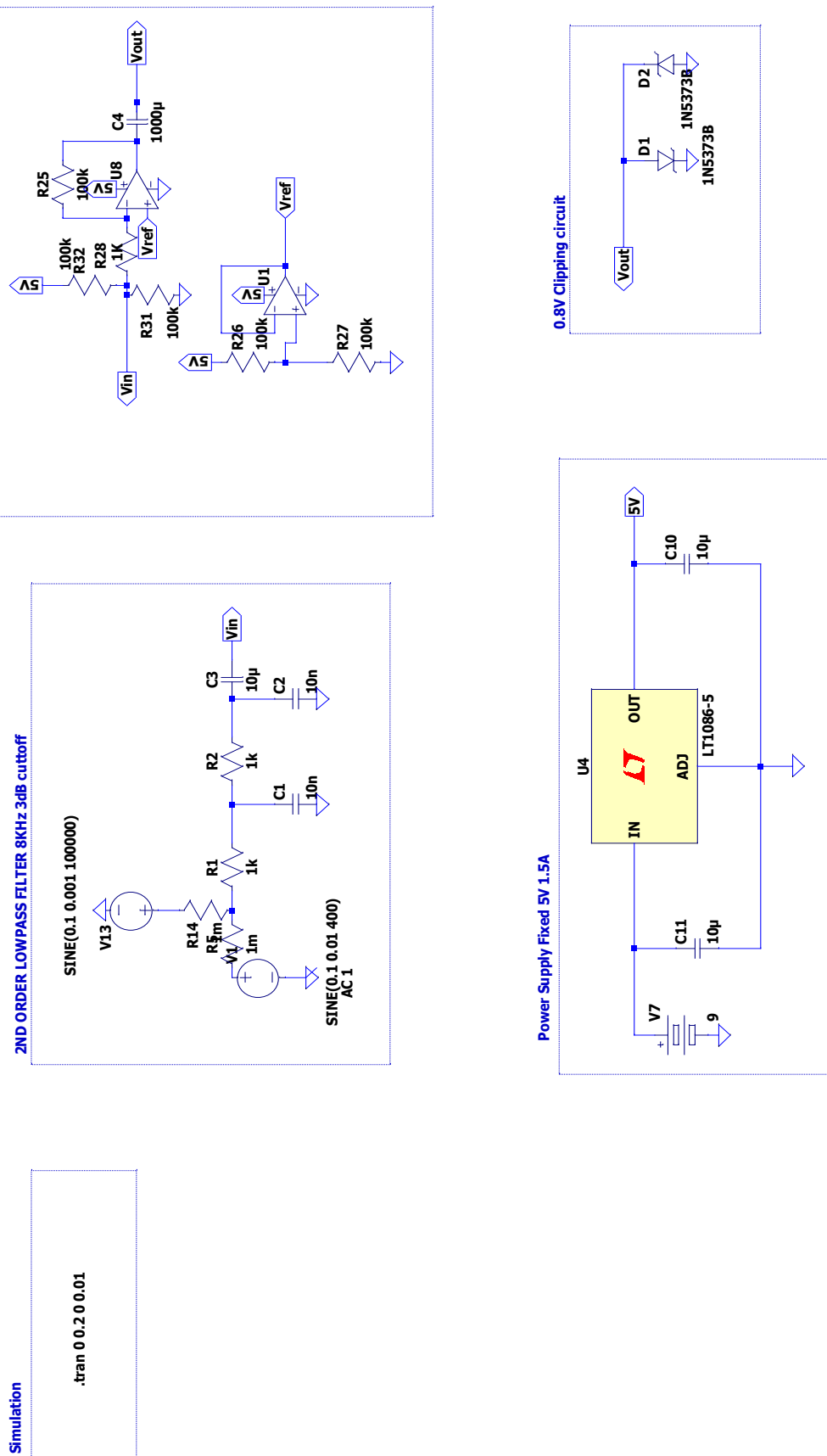


Figure F.2: Frequency Response of Lowpass Filter

**Figure F.3:** LTSpice Simulation of Radar Hardware

The radar software was tested by simulating a sine wave in Matlab with a frequency of 1000 Hz, with added Gaussian noise. The signal is simulated to be sampled with a frequency of 44 100 Hz. The signal was imported into the radar software to test its capability to extract the speed. The spectrogram of the signal with the noise is shown in figure F.4 and the measured speed is shown in figure F.5.

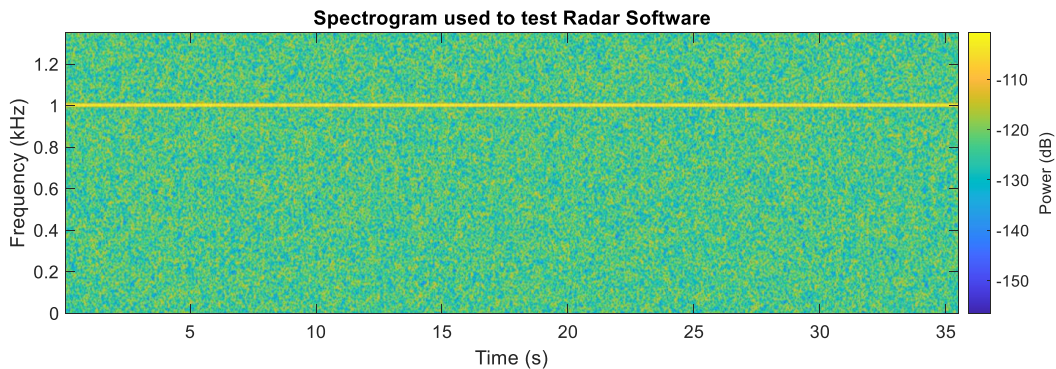


Figure F.4: Spectrogram of Simulated Signal

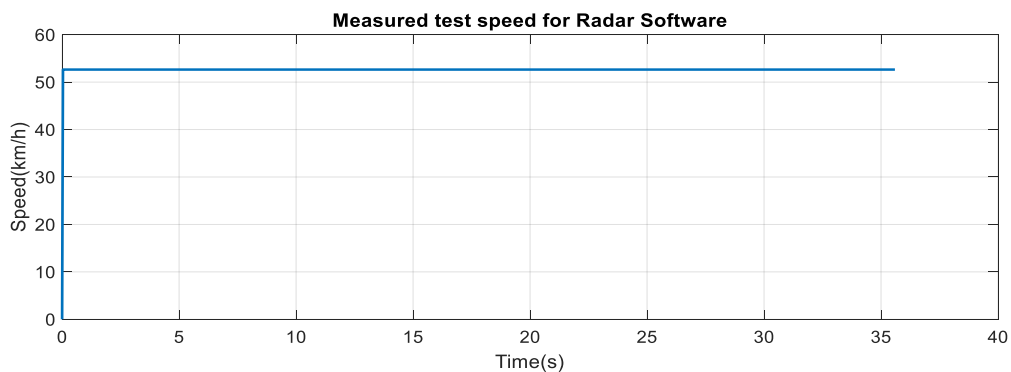


Figure F.5: Measured Speed from Simulated Signal

Appendix G

Spectrograms regarding the Accuracy and Acceleration



Figure G.1: Spectrogram with best combination of Time and Frequency Resolution

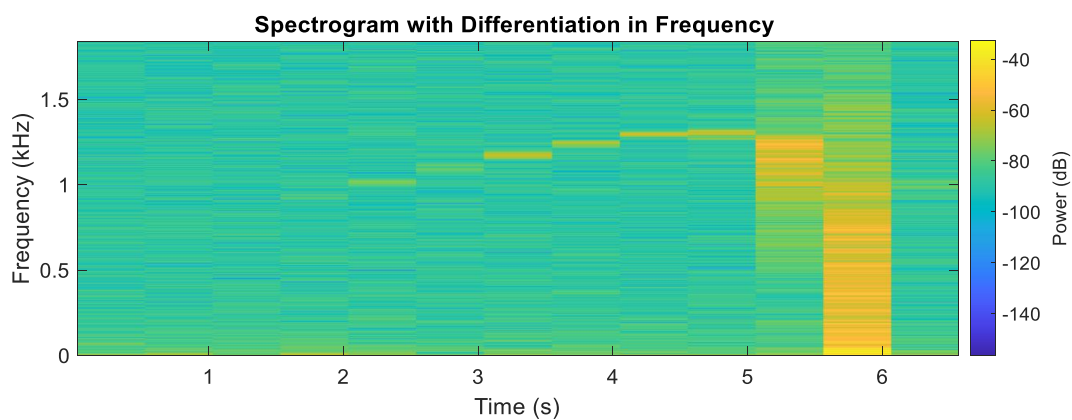


Figure G.2: Spectrogram with Differentiation in Frequency



Figure G.3: Spectrogram with Differentiation in Time

Appendix H

Spectrograms regarding the Antenna Sidelobe

The spectrograms below are from measurements with the HB100 sensor before adding the horn antenna. Take note of the radiation pattern of the HB100 antenna, illustrated in figure E.1.

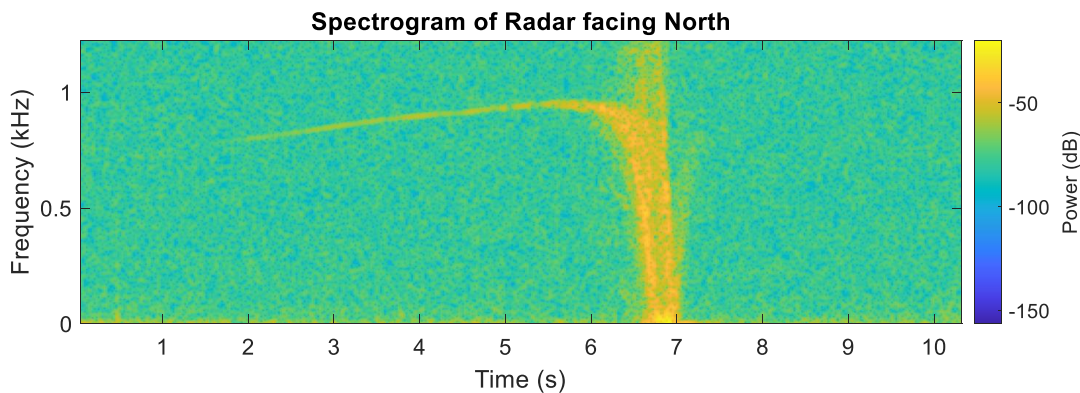


Figure H.1: Spectrogram of Radar facing North

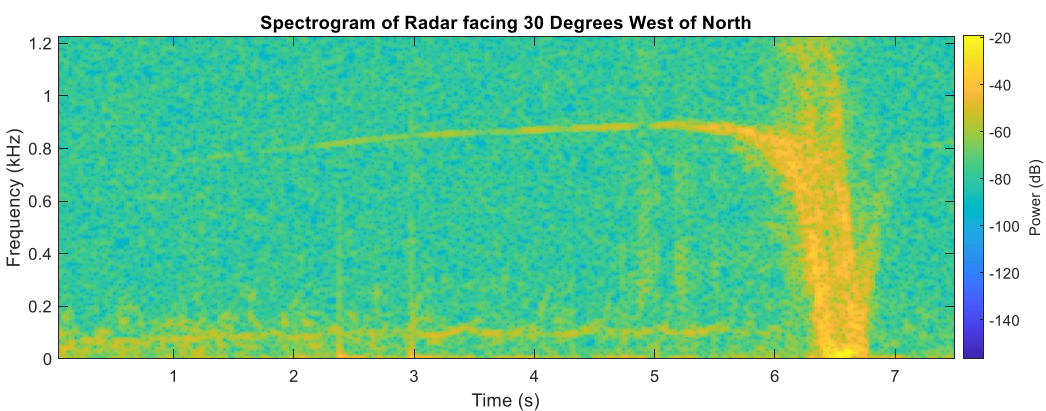


Figure H.2: Spectrogram of Radar facing 30 Degrees West of North

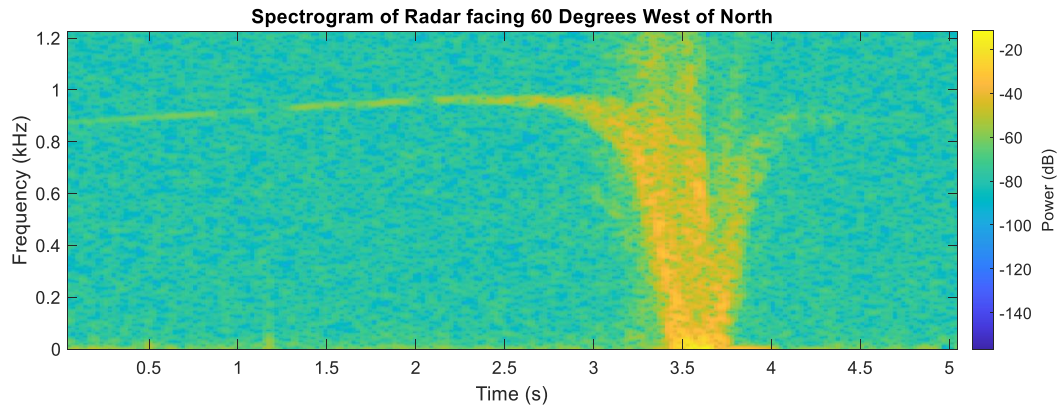


Figure H.3: Spectrogram of Radar facing 60 Degrees West of North

The next set of spectrograms was measured after the addition of the horn antenna. The radiation pattern of the horn antenna added to the radar is illustrated in figure E.4.

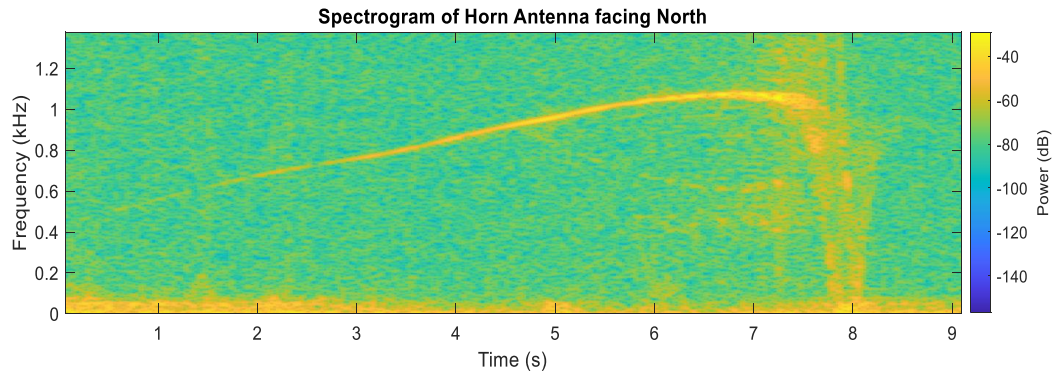


Figure H.4: Spectrogram of Radar facing 0 Degrees West of North

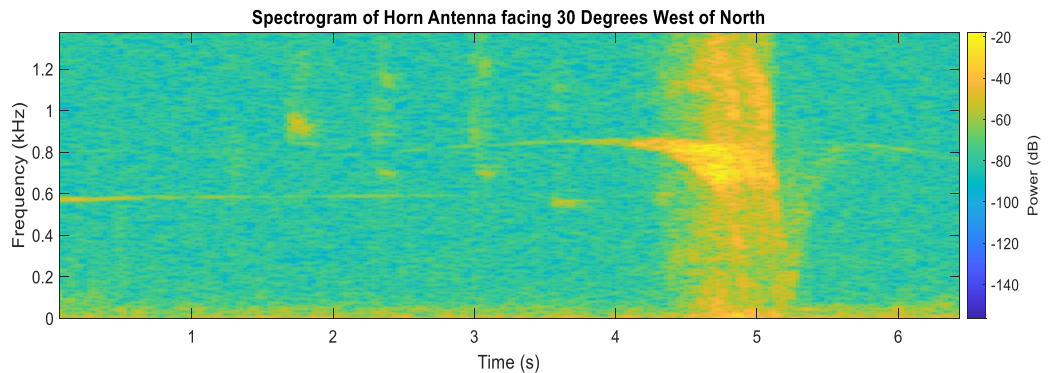


Figure H.5: Spectrogram of Radar facing 30 Degrees West of North

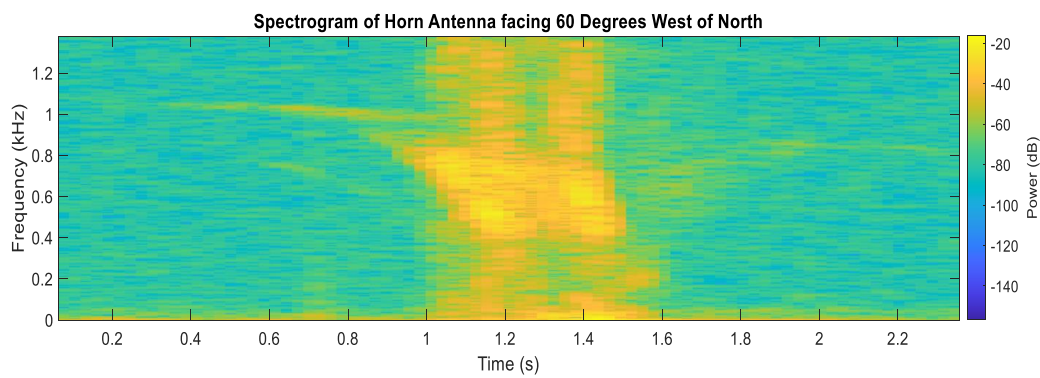


Figure H.6: Spectrogram of Radar facing 60 Degrees West of North

Appendix I

Matlab Code

```
1 % PARAMETER FILE
2 % READ DATA IN FROM WAV FLIE
3 [y,Fs] = audioread('multipathHORN1.wav');
4 % DOWNSAMPLE MEASURMENT
5 downSampleRate =16;
6 y = downsample(y,downSampleRate);
7 Fs = Fs/downSampleRate;
8 % DFT LENGTH AND OVERLAP
9 Length=300;
10 timeStep=Length/Fs;
11 overlap=0.3;
12 % DFT FRAME SETUP
13 frames = round(size(y)/Length);
14 frames = frames(1)-1;
15 startFrame=1;
16 endFrame=frames;
17 % CREATE EMPTY ARRAYS FOR SPEED MEASUREMENT
18 speed = zeros(frames,1);
19 tracked_speed1 = [0 0];
20 sample_Array = zeros(Length,1);
21 % CREATE VARIABLES FOR SPEED AND SPEED LIMITS
22 frequency=0;
23 speed=0;
24 speedLimit=10;
25 % CREATE FREQUENCY BIN RANGE
26 bins = ((timeStep)^2*(1-overlap))*175.41;
27 % TRACKING FLAG
28 tracked=0;
29 % RADAR DISTANCES
30 d=3;
31 R=0;
32 % COSINE ANGLE
33 cosineAngle=0;
34 %SNR SCALER
35 scale=1;
```

```

1 %SPEED ALGORITHM
2 %STFT CALCULATION
3 for n=startFrame:1:(endFrame/(1-overlap))
4     max_FFT_index=0;
5     max_FFT=0;
6     s=[0 0];
7     s_index=[0 0];
8     num=1;
9     SNR_Average=0;
10    % POPULATE A FRAME
11    for b = 1:1:Length
12        sample_Array(b)=y(b+Length*(n-1)-(overlap*Length)*(n-1));
13    end
14    % CALCULATE DFT OF FRAME
15    g=abs(fft(sample_Array));
16    % DETERMINE MAX DFT INDEX
17    for x = 1:1:Length/2
18        if max_FFT<g(x)
19            max_FFT=g(x);
20            max_FFT_index=x;
21        end
22    end
23    % DYNAMIC SNR CALCULATION
24    for x = 1:1:Length
25        SNR_Average = SNR_Average + g(x);
26    end
27    SNR_Average = SNR_Average/Length;
28    for x = 1:1:Length
29        if g(x)>(SNR_Average)
30            s(num)=g(x);
31            s_index(num)=x;
32            num=num+1;
33        end
34    end
35    for x = 1:1:length(s)
36        SNR_Average = SNR_Average + s(x);
37    end
38    SNR = (SNR_Average/length(s))*scale;
39    % CHECK IF MAX FREQUENCY COMPONENT IS GREATER THAN SNR LEVEL
40    if max_FFT>SNR
41        % CONVERT DFT INDEX TO SPEED
42        speed_kmh=(max_FFT_index*Fs/Length)/19.49;
43        if speed_kmh≥speedLimit
44            speed(n)=speed_kmh;
45        end
46    end
47 end

```

```

1 %TRACKING OF A SINGLE VEHCILE
2 for n=startFrame:1:(endFrame/(1-overlap))
3     z=[0 0];
4     p=0;
5     s=[0 0];
6     s_index=[0 0];
7     num=1;
8     SNR_Average=0;
9     max_FFT_index=0;
10    max_FFT=0;
11    sample_Array = [0 0];
12    % POPULATE A FRAME
13    for b = 1:1:Length
14        sample_Array(b)=y(b+Length*(n-1)-(overlap*Length)*(n-1));
15    end
16    % CALCULATE DFT OF FRAME
17    g=abs(fft(sample_Array));
18    % DETERMINE MAX DFT INDEX
19    for x = 1:1:Length/2
20        if max_FFT<g(x)
21            max_FFT=g(x);
22            max_FFT_index=x;
23        end
24    end
25    % DYNAMIC SNR CALCULATION
26    for x = 1:1:Length
27        SNR_Average = SNR_Average + g(x);
28    end
29    SNR_Average = SNR_Average/Length;
30    for x = 1:1:Length
31        if g(x)>(SNR_Average)
32            s(num)=g(x);
33            s_index(num)=x;
34            num=num+1;
35        end
36    end
37    for x = 1:1:length(s)
38        SNR_Average = SNR_Average + s(x);
39    end
40    SNR = (SNR_Average/length(s))*scale;
41    % CHECK IF MAX FREQUENCY COMPONENT IS GREATER THAN SNR LEVEL
42    if max_FFT>SNR
43        % CHECK IF MAX FREQUENCY COMPONENT IS WITHIN BIN RANGE
44        if abs(frequency-max_FFT_index)≤round(bins)
45            % CONVERT DFT INDEX TO SPEED
46            speed=(frequency*Fs/Length)/19.49;
47            if speed>speedLimit

```

```

48         tracked_speed1(n)=speed;
49     end
50 else
51     speed=0;
52 end
53 end
54 frequency=max_FFT_index;
55 end
56 % CALCULATE TIME JUMP PER FRAME
57 time = zeros(1,length(tracked_speed1));
58 for x=1:1:length(tracked_speed1)
59     time(x) = (x-1)*(Length/Fs)*(1-overlap);
60 end
61 % PLOT THE TRACKED SPEED
62 plot(time,tracked_speed1);
63 title('Tracked Speed');
64 xlabel('Time(s)');
65 ylabel('Speed(km/h)');
66 grid on;
67 % CALCULATE TOTAL DISTANCE VEHICLE IS TRACKED
68 for x=1:1:size(tracked_speed1)
69     distance=distance+tracked_speed1(x)*timeStep/3.6*(1-overlap);
70 end

```

```

1 %GENERATE SPECTROGRAM
2 signal=y;
3 filter = hann(428);
4 overlap=350;
5 windowSize = 8192;
6 spectrogram(signal,filter,overlap,windowSize,Fs,'power','yaxis');

```

```

1 %COSINE ANGLE CORRECTION FOR A SINGLE TRACKED VEHICLE
2 R=distance;
3 cosineCorrectedSpeed=tracked_speed1;
4 for x=1:1:size(tracked_speed1)
5     % ESTIMATE OF HOW FAR VEHICLE IS FROM RADAR
6     R = R - (timeStep*(1-overlap))*(cosineCorrectedSpeed(x-1)/3.6);
7     if R>d
8         % CALCULATE COSINE ANGLE
9         cosineAngle=atand(d/R);
10    end
11    % CORRECT SPEED
12    cosineCorrectedSpeed(x) = cosineCorrectedSpeed(x)/cosd(cosineAngle);
13 end
14 plot(time,cosineCorrectedSpeed);

```